Prog. Biophys. molec. Biol., Vol. 53, pp. 153–196, 1989.
Printed in Great Britain. All rights reserved.

0079–6107/89 $0.00+.50
© 1990 Pergamon Press plc

PREDICTIONS OF DIFFUSION MODELS FOR ONE-ION MEMBRANE CHANNELS

PETER GATES,* KIM COOPER,* JAMES RAE* and ROBERT EISENBERG†

**Departments of Physiology and Biophysics and Ophthalmology, Mayo Foundation, Rochester, MN 55905, U.S.A.*

†*Department of Physiology, Rush Medical College, Chicago, IL 60612, U.S.A.*

CONTENTS

SYMBOLS AND ABBREVIATIONS

Greek symbols

δ	Length of the channel
$\Delta\phi$	Difference in dimensionless potential across the membrane
ξ	Dimensionless length defined in Fig. 3, panel 5
τ_l	Mean first passage time with an initial position and reflecting boundary at $x=-\delta/2$ and an absorbing boundary at $x=\delta/2$
τ_r	Mean first passage time with an initial position and reflecting boundary at $x=\delta/2$ and an absorbing boundary at $x=-\delta/2$
ϕ	Dimensionless potential energy
$\phi^0(x)$	Dimensionless ion–channel interaction potential
$\Delta\phi_{1/2}$	Dimensionless voltage at which J_{is} reaches 1/2 its saturation value
$\Delta\phi^0$	$\phi^0(\delta/2)-\phi^0(-\delta/2)$
β_p	Defined in eqn (A35) in Appendix 1

JPB 53-3-A

β_n Defined in eqn (A36) in Appendix 1
γ_p Defined in eqn (A35) in Appendix 1
γ_n Defined in eqn (A36) in Appendix 1

English symbols
A Cross sectional area of the channel
D Diffusion coefficient (m^2/sec)
G Small signal conductance of a channel (Siemens)
G_i Small signal conductance in the independence case
G_s Small signal conductance in the saturation case
J Flux through a channel (ions/sec)
J_i Flux through a channel under the assumption of independence
J_{iss} Small signal independence flux
J_{ia} Independence flux with access limitations
K_{al} Affinity constant for ions entering the left end of the channel
K_{ar} Affinity constant for ions entering the right end of the channel
k_b Boltzmann's constant (1.38×10^{-23} joules/kelvin)
n Density of ions (ions/m^3)
$\bar{n}$ $\sqrt{n(-\infty)n(\infty)}$
$n(\infty)$ Concentration of ions in right bath far from channel mouth
$n(-\infty)$ Concentration of ions in left bath far from channel mouth
$n(\delta/2)$ Concentration of ions at the right mouth of the channel
$n(-\delta/2)$ Concentration of ions at the left mouth of the channel
R_a^b Electrodiffusive resistance between points a and b (sec/m^3)
R_l Electrodiffusive resistance of the left bath
R_r Electrodiffusive resistance of the right bath
R_c Electrodiffusive resistance of the channel
R_t Total electrodiffusive resistance of system
r_n $n(\infty)/n(-\infty)$
r $\frac{1}{2} \ln r_n$
T Absolute temperature
t_l Average time spent in the channel by an ion entering from the left bath
t_r Average time spent in the channel by an ion entering from the right bath
z Valence of an ion

List of abbreviations
MFPT Mean first passage time
MOT Mean occupancy time

I. INTRODUCTION

In recent years, the study of channels has become a vast and varied field of study. Our knowledge of channel function has increased at all levels. At the tissue level, it is now recognized that channels are involved in several important disease processes (reviewed in Andreoli *et al.*, 1986), with cystic fibrosis being a recent notable example (Frizzell, 1987; Welsh and Fick, 1987; Riordan *et al.*, 1989). At the cellular level, channels are now known to be involved in everything from cell volume regulation to the control of mitogenesis (Hoffmann and Simonsen, 1989; Pandiella *et al.*, 1989; Frace and Gargus, 1989). At the molecular level, channels are being studied with sophisticated new biophysical and molecular biological techniques (Numa, 1989).

We recognize three fundamental aspects of channel function: gating, permeation, and regulation. Our theoretical understanding of the first two processes is changing rapidly. The theory of channel gating has reached new levels of sophistication and new approaches are being developed (Liebovitch *et al.*, 1987; Millhauser *et al.*, 1988; Lauger, 1988; Levitt, 1989). In the area of permeation theory, recent developments include the reintroduction of diffusion theory to describe ion movements through channels (Levitt, 1986, 1987; Jackobsson and Chiu, 1987; Cooper *et al.*, 1988a,b; Gates *et al.*, 1990).

Ever since the work of Hodgkin and Keynes (1955), it has been recognized that ions interact strongly with each other as they move through a channel. Since that realization, it has become customary to classify channels (and models of channels) in two categories, single-ion channels and multi-ion channels. The number of channels that do not show some deviation from single-ion behavior has steadily decreased. Thus is seems that the single-ion channel may be more a convenient fiction than a reality. However, single-ion models allow

relatively simple analytical results and therefore are a convenient starting point for theoretical understanding of channel behavior. It is in this spirit that we present an analysis of a single-ion channel model based on diffusion theory.

The goal of our analysis will be to understand the behavior of the current through a one-ion channel as a function of the permeant ion concentration, the applied transmembrane voltage and most importantly the intrinsic ion–channel interaction potential. Three major themes will be developed. First, we will analyze the effects of bath access limitations for a one-ion diffusion model. Several approaches to this problem have been presented for rate theory models (Lauger, 1976; Hladky, 1984; Sandblom, 1985). Second, we will discuss three mechanisms of rectification for a one-ion channel. These include: the standard Goldman type concentration difference rectification, rectification due to a difference in the potential between the bath and the channel mouth, and rectification due to a nonzero slope in the interaction potential at the mouths of the channel. The last theme has to do with a difference between diffusion models and Eyring models. It appears to be a general result that diffusion models give rise to more linear current–voltage relationships than do the corresponding Eyring models. We will discuss the nature of this linearity.

We are aware of a number of limitations in the theory we present here. The most important limitation is the assumption of single-ion occupancy. In the discussion we will present an approximate equilibrium method for determining how good the single-ion assumption is for a given potential profile. Another limitation is the assumption that the ion channel interaction potential is static. This is equivalent to assuming that relaxation of the average channel structure in response to the electrical field produced by the ion is fast relative to the time scale of the movement of the ion in the channel. In general this may not be true and the potential may depend on such things as the fraction of time the channel is occupied (Lauger, 1985) and the details of a particular ion's movement in the channel (Edmonds, 1989). There are in addition several assumptions made in developing the theory that may not be obvious to the reader. We will mention these briefly. Finally, we will discuss the future of analytical diffusion models for ion permeation.

II. OUTLINE OF ONE-ION DIFFUSION THEORIES

1. *Boundary Conditions for One-Ion Diffusion Theories*

Three methods have been suggested in the literature for specifying the boundary conditions of the Nernst–Planck equation. Levitt (1982) obtained boundary conditions by invoking virtual binding sites at the ends of the channel which exchanged with the bath according to a set of rate constants. This work motivated a formulation involving a kinetic scheme whose rate constants were specified by solving diffusion equations with absorbing and reflecting boundaries (Gates *et al.*, 1990). These two formulations are essentially equivalent and can be considered to be hybrids of rate theory models and diffusion models. The second approach was first suggested by Levitt (1986). In this formulation the boundary concentrations of the Nernst–Planck equation were obtained by assuming that the ends of the channel were at equilibrium with the bath concentrations. This was later generalized to the two ion case (Levitt, 1987). The third (C–J) approach (Chiu and Jakobsson, 1989) was to assume a steady state flux in the bath that was independent of channel occupancy. Combining this assumption with Levitt's (1986) results yielded a quadratic equation in the flux.

The physical consequence of these three approaches is the way in which access limitations are handled. The simplest of the three is Levitt's (1986) method in which access limitations are assumed negligible. The other two methods are attempts to include access limitations. The hybrid method is an extension of the traditional rate theory approaches and is fundamentally of the same form as the equilibrium boundary conditions. The hybrid approach has the disadvantage that it overestimates access effects at high concentrations. We will return to this issue in Section IV. The C–J boundary conditions are qualitatively superior to the hybrid method because at high concentrations access effects become negligible and the equilibrium boundary conditions are recovered. This approach still suffers

from a failure to properly handle interactions between an ion in the channel and ions in the bath (see Summary and Discussion of Chiu and Jakobsson, 1989). A proper treatment of the access problem must involve the pairwise interactions of many ions simultaneously.

In the following sections we will derive both the hybrid model and the model proposed by Chiu and Jakobsson. We will then describe the numerical consequences of the hybrid approach with most of the emphasis on the negligible access limit which is a common special case of both methods (for numerical results of the C–J boundary conditions see Chiu and Jakobsson, 1989).

(a) *Hybrid model*

We first describe a one-ion channel in terms of occupancy states and the rates of transition between those states. This allows us to write an expression for the flux* through the channel in terms of the transition rates. We then use diffusion theory to specify these transition rates in terms of the properties of the channel. Finally, we develop some conceptual tools to help understand the behavior of this model.

A one-ion channel can exist in one of three states (Fig. 1). It can have no ion in it (denoted

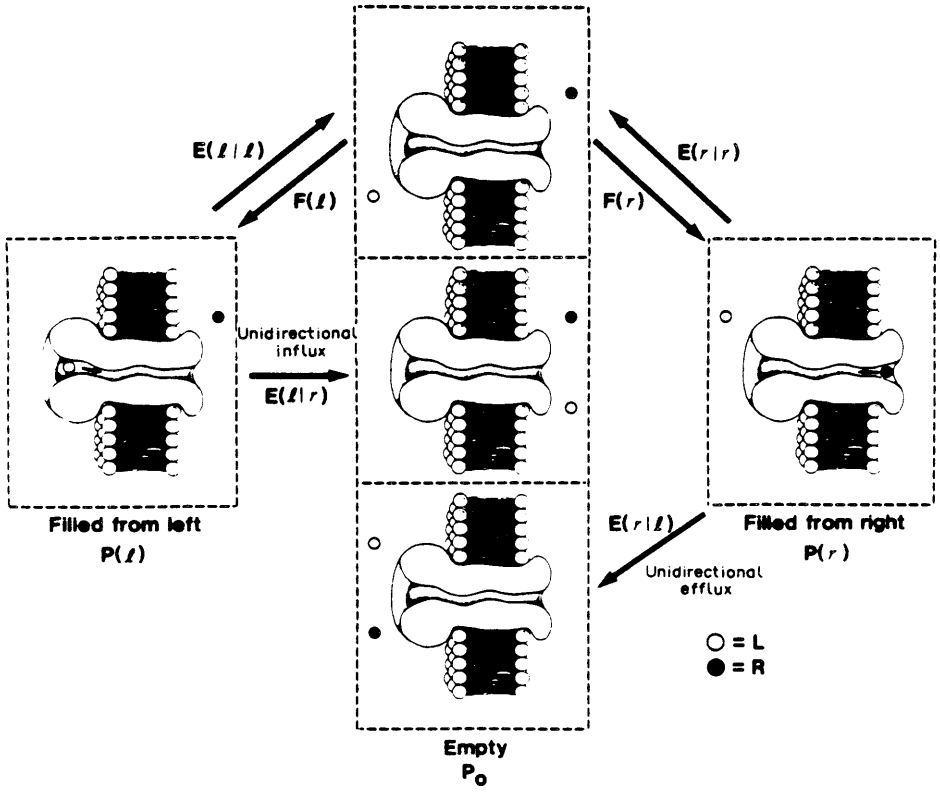

FIG. 1. Kinetic scheme. The three possible occupancy states of a one-ion channel and the transition rates between the states. P_0 is the probability that the channel is empty. $P(l)$ and $P(r)$ are probabilities of occupancy by ions from the left and right respectively. $F(l)$ and $F(r)$ are the filling rates for ions from the left and right baths respectively. $E(l|l)$ and $E(r|r)$ are the rates at which ions exit the same side they enter. $E(l|r)$ and $E(r|l)$ are the rates at which ions exit the opposite side they enter.

P_0), it can be occupied by an ion that entered from the left bath (denoted $P(l)$) or it can be occupied by an ion that entered from the right bath (denoted $P(r)$). These three states interconvert with the six rates shown in Fig. 1 and defined in the figure caption. A net flux (J) of ions through the channel from left to right occurs when the left-to-right flux is not balanced

*Flux is related to current by $I=zeJ$. We use flux instead of current to avoid unnecessary constants in our expressions.

by the right-to-left flux. This can be expressed in terms of the rates and occupancy probabilities as follows:

$$J = E(l|r)P(l) - E(r|l)P(r). \tag{1}$$

Expressions for the occupancy probabilities in terms of the rates can be obtained by standard kinetic techniques. The results are listed below.

$$P_0 = \frac{E(l)E(r)}{E(l)E(r) + F(l)E(r) + F(r)E(l)} \tag{2}$$

$$P(l) = \frac{F(l)E(r)}{E(l)E(r) + F(l)E(r) + F(r)E(l)} \tag{3}$$

$$P(r) = \frac{E(l)F(r)}{E(l)E(r) + F(l)E(r) + F(r)E(l)} \tag{4}$$

The following definitions have been made for convenience:

$$E(l) = E(l|l) + E(l|r) \tag{5}$$

$$E(r) = E(r|r) + E(r|l). \tag{6}$$

Equation (1) can be put in an alternate form by writing $P(l)$ and $P(r)$ in terms of P_0 and the transmission probabilities P_{lr} and P_{rl}. The transmission probabilities express the probability that an ion entering a given side of the channel successfully makes it through to the opposite bath. P_{lr} and P_{rl} are defined as follows:

$$P_{lr} = E(l|r)/E(l) \tag{7}$$

$$P_{rl} = E(r|l)/E(r). \tag{8}$$

In terms of these quantities the flux can be written:

$$J = P_0[F(l)P_{lr} - F(r)P_{rl}]. \tag{9}$$

Note that eqns (1) and (9) are complementary ways of saying the same thing. In both cases, the net flux is the difference between two unidirectional fluxes. Each unidirectional flux in eqn (1) is the product of the probability the channel is occupied by an ion from a given side and the rate at which that ion exits the opposite side. In eqn (9), each unidirectional flux is the product of the rate of entry of an ion to a given side (e.g. $P_0F(l)$) and the probability the ion exits the opposite side. Thus we have a choice as to whether we think about flux in terms of transmission probabilities and entrance rates, or in terms of entrance probabilities and transmission rates.

The effects of ion–ion interaction are contained in the P_0 term. It is this term that gives rise to the saturation of flux or conductance with increasing permeant ion concentration. Therefore the bracketed term in eqn (9) represents the flux that would exist in the absence of ion–ion interactions. We refer to it as the independence flux and denote it J_i. We will see the use of defining such a quantity later.

Equation (9) is a complete specification of the behavior of a one-ion channel. However, to do detailed calculation requires that the six rates be specified in terms of the bath ion concentrations, the applied voltage difference across the channel, and the potential energy profile seen by an ion as it traverses the channel. There are two ways of doing this. Traditionally the specification of the rates is made via transition state rate theory (Lauger, 1973). It is also possible to make the specification using a diffusion theory (Gates *et al.*, 1990; Cooper *et al.*, 1988a,b), and that is the approach we develop here.

The six rates are calculated by solving a set of diffusion problems with boundary conditions appropriate to each rate in the kinetic scheme. The diffusion equation we use is one dimensional and can be written:

$$-J = D(x)A(x)\left[\frac{dn}{dx} + n\frac{d\phi}{dx}\right], \tag{10}$$

where $A(x)$ is the area, $D(x)$ is the diffusion coefficient, n is the ion concentration in particles per unit volume, and ϕ is the dimensionless potential (i.e. the real potential divided by k_bT). ϕ contains both the applied voltage ($\Delta\phi$) and the intrinsic ion–channel interaction potential ($\phi^\circ(x)$). In the steady-state, eqn (10) can be integrated between two points a and b to yield:

$$-J = \frac{n(b)e^{\phi(b)} - n(a)e^{\phi(a)}}{\int_a^b \frac{e^{\phi(x)}dx}{A(x)D(x)}}. \tag{11}$$

The denominator of this expression occurs so frequently we give it a special symbol R_a^b, and refer to it as the electrodiffusive resistance. It has the units of the inverse of the product of permeability and area. Equation (11) has the form of a driving force divided by a resistance and is thus analogous to Ohm's law. The system we will be dealing with consists of a channel separating two semi-infinite baths. We choose the zero point of the x axis to be in the center of the channel. The channel is of length δ. Thus $R_{-\infty}^{-\delta/2}$ is the electrodiffusive resistance of the left bath, $R_{\delta/2}^{\infty}$ is the electrodiffusive resistance of the right bath, and $R_{-\delta/2}^{\delta/2}$ is the electrodiffusive resistance of the channel. We will use a somewhat more compact notation, using R_l, R_r, and R_c for the left bath, right bath and channel electrodiffusive resistances respectively. We denote the sum of these three resistances R_t.

The derivations of the rates from the diffusion equation are lengthy and the interested reader is referred to Gates *et al.* (1990) for details. In that paper, it is shown that the exit rate constant expressions can be written and understood in terms of the electrodiffusive resistances and a pair of times related to the lifetime of an ion occupancy event. We call these times mean occupancy times (MOT). They are a generalization of the mean first passage times (MFPT) used in the theory of diffusion processes (Goel and Richter-Dyn, 1974; Gardiner 1983). There are two such times in this model. One (t_l) corresponds to ions entering the left end of the channel and the other (t_r) is the analog for ions entering the right end of the channel. The six rates of the one-ion model are given in terms of these quantities below:

$$F(l) = \frac{n(-\infty)e^{-\Delta\phi/2}}{R_l} \tag{12}$$

$$F(r) = \frac{n(\infty)e^{\Delta\phi/2}}{R_r} \tag{13}$$

where $n(\infty)$ and $n(-\infty)$ are the concentrations in the right and left baths respectively at distances far from the channel mouths. Notice that if the potential in the electrodiffusive resistance is a superposition of the applied transmembrane voltage and a potential that is independent of the transmembrane voltage the filling rates become voltage independent. These equations for the entrance rates have an intuitive interpretation. The numerator of each rate is the driving force to the mouth of an empty channel. The denominator is the electrodiffusive resistance of the bath.

$$E(l|l) = \frac{R_c + R_r}{R_t}\left[\frac{1}{t_l}\right] \tag{14}$$

$$E(l|r) = \frac{R_l}{R_t}\left[\frac{1}{t_l}\right] \tag{15}$$

$$E(r|r) = \frac{R_c + R_l}{R_t}\left[\frac{1}{t_r}\right] \tag{16}$$

$$E(r|l) = \frac{R_r}{R_t}\left[\frac{1}{t_r}\right] \tag{17}$$

$$t_l = \frac{R_l}{R_t}\left[\tau_l + \frac{R_r}{R_c}(\tau_l + \tau_r)\right] \tag{18}$$

$$t_r = \frac{R_r}{R_t}\left[\tau_r + \frac{R_l}{R_c}(\tau_l + \tau_r)\right] \tag{19}$$

Here τ_l is the MFPT for an ion which is initially at the left end of the channel and reflecting and absorbing boundaries at the left and right ends of the channel respectively. τ_r is the analogous MFPT for an ion initially at the right end of the channel.

The form of the exit rates can also be given a simple interpretation. Note that by combining eqns (14) and (15), $E(l) = 1/t_l$ and $E(r) = 1/t_r$. Thus the total rate of exit for ions entering from a given side is the inverse of the occupancy time for those ions. If we think of the exit rates as currents and the electrodiffusive resistances as electrical resistances, eqns (14) through (17) are just statements of current division. This means that an ion sitting at the mouth of the channel "makes a decision" whether to go through the channel or back into the bath based on the relative electrodiffusive resistances in the two directions. The equation for $E(l|r)$ can be understood as follows. If the channel resistance is much larger than the bath resistance, the ratio R_r/R_c in t_l goes to zero. In that case, $E(l|r)$ is equal to the inverse of the MFPT through the channel. This is almost a tautology. The inverse of this exit rate is by definition the mean time it takes an ion to traverse the channel and that is essentially what the MFPT expresses. In such a situation, when an ion leaves the channel, the chances of it reentering before it diffuses away become negligible. Thus the second term in t_l represents the effect of reentrances. These reentrances decrease the rate as would be expected. An analogous argument holds for $E(r|l)$.

The MFPTs (τ_l and τ_r) depend only on the dimensionless potential $\phi(x)$, the channel diffusion constant (D) which is contained in the electrodiffusive resistance, and the length of the channel (δ), as given in the following equations:

$$\tau_l = A\int_{-\delta/2}^{\delta/2} R_x^{\delta/2} e^{-\phi(x)}\,dx \tag{20}$$

$$\tau_r = A\int_{-\delta/2}^{\delta/2} R_{-\delta/2}^{x} e^{-\phi(x)}\,dx. \tag{21}$$

Here, we have introduced an electrodiffusive resistance with a variable region of integration. For example:

$$R_x^{\delta/2} = \frac{1}{AD}\int_x^{\delta/2} e^{(\phi\xi)}\,d\xi. \tag{22}$$

As discussed above, τ_l and τ_r can be interpreted as the mean time a channel is occupied per ion transported for the special case of negligible bath access resistances (see also Jakobsson and Chiu, 1987). The relationship between a MFPT and this mean transport time is discussed at some length in Gates *et al.* (1990).

The above equations can now be combined with eqns (2), and (5–9) to yield an equation for J in terms of the concentrations, transmembrane voltage, and ion–channel interaction potential. This yields the following general form of the one-ion diffusion model.

$$J = \frac{n(-\infty)e^{-\Delta\phi/2} - n(\infty)e^{\Delta\phi/2}}{R_t\left[1 + n(-\infty)\frac{t_l}{R_l} + n(\infty)\frac{t_r}{R_r}\right]} \tag{23}$$

The numerator in eqn (23) is the driving force written in symmetrical form. It is the difference in the exponential of the electrochemical potential between the two baths. In the denominator, the second and third terms represent the effect of ion–ion interaction. It is these terms that cause the flux to saturate with increasing permeant concentration. If the concentration on both sides of the channel is small enough, these terms are negligible and the

denominator becomes the total electrodiffusive resistance and we have the independence flux. If the bath resistances are negligible in comparison to the channel resistance, R_t becomes R_c, t_l/R_l becomes $\tau_l e^{-\Delta\phi/2}/R_c$ and t_r/R_r becomes $\tau_r e^{\Delta\phi/2}/R_c$. In this situation eqn (23) reduces to the result derived by Levitt (1986).

(b) *Chiu–Jakobsson one-ion diffusion model*

In our notation eqn (2) of Chiu and Jakobsson (1989) becomes:

$$-J=\frac{P_0}{R_c}[n(a)e^{\phi(a)}-n(-a)e^{\phi(-a)}]. \tag{24}$$

This equation can be interpreted as the product of the flux through the channel under the assumption of independence and the probability the channel is empty. That is, an ion at the capture radius a can enter the channel only if the channel is empty. Levitt (1986) suggests that the concentration at the capture radius can be related to the bath concentration through the Boltzmann distribution. For example on the left end of the channel $n(-a)e^{\phi(-a)}=n(-\infty)e^{\phi(-\infty)}$. Chiu and Jakobsson suggest as an alternative that the Boltzmann distribution be replaced by a steady state diffusion equation in the radial coordinate. In our notation we have, solving for the concentration at the capture radius:

$$n(-a)e^{\phi(-a)}=n(-\infty)e^{-\Delta\phi/2}-JR_l \tag{25}$$

$$n(a)e^{\phi(a)}=n(\infty)e^{\Delta\phi/2}+JR_r. \tag{26}$$

In the hybrid model the flux in the bath is assumed to be zero when the channel is occupied. This assumption can be incorporated into eqns (25) and (26) by dividing the flux by P_0. Although the one-ion assumption does imply that the rate at which ions enter the channel is zero when the channel is occupied it does not follow that the flux in the bath is zero when the channel is occupied. In fact, as an ion moves through the channel the electric field in the bath changes producing a displacement current (see Levitt, 1985). In the absence of such a modification eqns (25) and (26) imply that the flux in the bath is independent of the channel occupancy. Combining eqns (24) through (26) yields an equation for the flux in terms of the empty probability and the concentrations in the bath:

$$-J[R_c+P_0(R_r+R_l)]=P_0[n(\infty)e^{\Delta\phi/2}-n(-\infty)e^{-\Delta\phi/2}]. \tag{27}$$

A closed form solution only requires an expression for the empty probability. Making use of our notation after some rearrangement Levitt's (1986) result for P_0 becomes:

$$P_0=\left\{1+\frac{1}{R_c}[n(-a)e^{\phi(-a)}\tau_l+n(a)e^{\phi(a)}\tau_r]\right\}^{-1}. \tag{28}$$

Again we make use of eqns (25) and (26) to obtain an expression in terms of the bath concentrations and the flux:

$$P_0=\left\{1+\frac{1}{R_c}[(n(-\infty)e^{-\Delta\phi/2}-JR_l)\tau_l+(n(\infty)e^{\Delta\phi/2}+JR_r)\tau_r]\right\}^{-1}. \tag{29}$$

Equations (27) and (29) are two equations in the two unknowns J and P_0. Inserting eqn (29) into eqn (27) and collecting terms yields an expression that is quadratic in the flux:

$$\alpha J^2+\beta J+\gamma=0$$

$$\alpha=\frac{1}{R_t}[\tau_r R_r-\tau_l R_l]$$

$$\beta=1+\frac{1}{R_t}[n(\infty)e^{\Delta\phi/2}\tau_r+n(-\infty)e^{-\Delta\phi/2}\tau_l]$$

$$\gamma=\frac{1}{R_t}[n(\infty)e^{\Delta\phi/2}-n(-\infty)e^{-\Delta\phi/2}]. \tag{30}$$

In the limit where the access resistances are negligible α goes to zero, R_t goes to R_c and we again recover Levitt's (1986) result.

2. *Conceptual Framework*

Our goal is to investigate the behavior of this one-ion channel model under conditions of varying transmembrane voltage and concentration. However, even this simple model is quite complex. To investigate its behavior systematically, we need some conceptual framework to guide us. Let us begin by considering those factors that determine the flux. The flux is a function of the ionic concentrations in the two baths, the intrinsic ion–channel interaction potential ($\phi^0(x)$) and applied transmembrane voltage ($\Delta\phi$), as follows:

$$J = F[n(-\infty), n(\infty), \quad \phi^0(x), \Delta\phi]. \tag{31}$$

The concentrations of ions in the baths and the transmembrane potential can be directly controlled and are thus key experimental parameters. We certainly need to understand how the model depends on them. However, one channel type is distinguished from another primarily by the ion–channel interaction potential. This potential can, in principle, be controlled by modifying the structure of the channel. This approach has been realized for several channels using site directed mutagenesis (for reviews see Dani, 1989; Krueger, 1989; Miller, 1989). The relationship between the structural properties of a channel and the ion–channel interaction potential is not well understood and thus we have little to guide us in our choice of $\phi^0(x)$. For this reason, we use several simple ion–channel interaction potentials. These have been chosen to illustrate some of the major factors in $\phi^0(x)$ that determine the flux.

We propose to characterize the flux by three quantities: the independence flux (J_i), the saturation flux (J_s), and the half saturation concentration ($n_{1/2}$). In the remainder of this section we discuss why these three quantities are useful. Equation (1) or (9) can be combined with eqns (2) through (8) to yield:

$$-J = \frac{n(\infty)e^{\Delta\phi/2} - n(-\infty)e^{\Delta\phi/2}}{R_t[1 + n(\infty)K_{ar} + n(-\infty)K_{al}]} \tag{32}$$

where

$$K_{al} = \frac{F(l)}{n(-\infty)E(l)} = \frac{t_l}{R_l}, \quad K_{ar} = \frac{F(r)}{n(\infty)E(r)} = \frac{t_r}{R_r}. \tag{33}$$

K_{al} and K_{ar} are the channel affinities for ions entering the left and right ends of the channel respectively. If we vary the magnitude of the concentration on one end of the channel while holding the ratio $r_n = n(\infty)/n(-\infty)$ fixed, the flux saturates with a hyperbolic form. The same is also true of the conductance. Since conductance saturation is often used experimentally, we have plotted in Fig. 2 the conductance of the one-ion model vs the magnitude of the concentration vector. The hyperbolic dependence of the conductance on the concentration can be characterized by two parameters: the saturation value of the conductance and the value of the concentration at half saturation ($n_{1/2}$). The saturation value is the largest conductance attainable for a given voltage and is achieved in the limit where the concentration goes to infinity holding r_n fixed. The half saturation concentration is the magnitude of the concentration vector for which the channel is occupied one half of the time. In order to produce expressions which are symmetric it is convenient to use the geometric average of the concentrations $\bar{n} = \sqrt{n(\infty)n(-\infty)}$. For the flux we can write:

$$J = \frac{\bar{n}J_s}{\bar{n}_{1/2} + \bar{n}} \tag{34}$$

$$J_s = \frac{1/\sqrt{r_n}\, e^{-\Delta\phi/2} - \sqrt{r_n}\, e^{-\Delta\phi/2}}{R_t[K_{al}/\sqrt{r_n} + K_{ar}\sqrt{r_n}]} \tag{35}$$

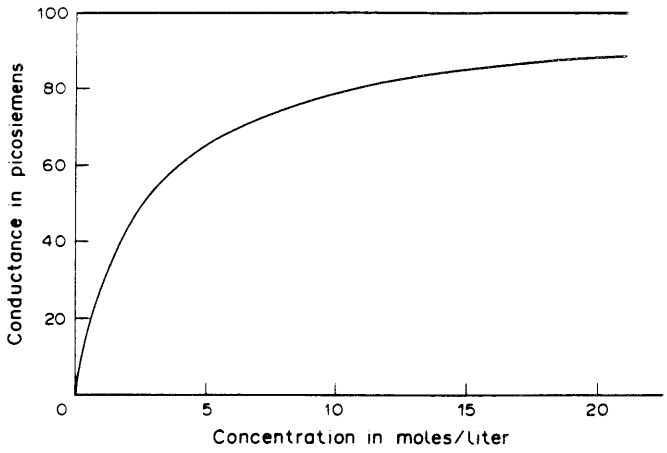

FIG. 2. Hyperbolic dependence of conductance vs concentration for a one-ion channel. Plot of the single channel conductance of a channel 5 nm in length, 0.2 nm in radius, ion–channel interaction potential identically zero and diffusion coefficient $0.4 \times 10^{-9} m^2/sec$. Half saturation concentration is the reciprocal of the channel volume and is 2.64 M. The saturation conductance $[e^2 D/(k_b T \delta^2)]$ is 100 pSiemens.

$$\bar{n}_{1/2} = \frac{1}{K_{al}/\sqrt{r_n} + K_{ar}\sqrt{r_n}} \tag{36}$$

$$J_i = \frac{1}{R_t}[n(-\infty)e^{-\Delta\phi/2} - n(\infty)e^{\Delta\phi/2}]. \tag{37}$$

From the above analysis we see that the flux increases linearly at low concentrations (as described by J_i), then bends over and approaches a limiting flux (J_s). The rate at which this occurs is determined by $\bar{n}_{1/2}$. We propose to understand this one-ion model by examining the dependence of the three quantities J_i, J_s, and $\bar{n}_{1/2}$ on $\Delta\phi$ and $\phi^0(x)$. We add that the C–J boundary conditions do not lead to a simple hyperbolic saturation of the conductance. In that model the conductance saturates to the value predicted when access limitations are negligible. Thus, at low concentrations, the flux for both models is given by the independence flux. At high concentrations the flux in the C–J model asymptotically approaches the hyperbola describing the saturation of the no access case.

III. INDEPENDENCE FLUX (J_i)

We begin our investigation of the behavior of the one-ion channel model by studying the dependence of J_i on the transmembrane potential $\Delta\phi$ and the intrinsic interaction potential $\phi^0(x)$. We will introduce the set of intrinsic interaction potentials used throughout the rest of the paper. We then investigate J_i in the absence of access resistance effects, i.e. when the bath resistances are much less than the channel resistance. At the end of this section the negligible access resistance assumption will be relaxed.

1. *Negligible Access Effects*

We now begin investigating the behavior of J_i. We will initially assume negligible access resistances. Under this assumption eqn (23) becomes:

$$-J_i = \frac{1}{R_c}[n(\delta/2)e^{\Delta\phi/2} - n(-\delta/2)e^{-\Delta\phi/2}], \tag{38}$$

where $n(\delta/2)$ and $n(-\delta/2)$ are the concentrations at the mouths of the channel. These concentrations are the same as those far from the mouths of the channel if the bath resistances are negligible. At this point we introduce two new parameters. Since $\Delta\phi/2$ occurs so ubiquitously we replace it by the letter u. To introduce symmetry into the two components of the driving force, we also introduce a dimensionless ratio for the concentrations as follows:

$$r=\tfrac{1}{2}\ln(r_n)=-\tfrac{1}{2}\ln[n(\infty)/n(-\infty)]. \tag{39}$$

In terms of these parameters eqn (38) is:

$$-J_i=\frac{2\bar{n}\sinh(u+r)}{R_c}. \tag{40}$$

We have defined the reference potential in our system such that electrical ground is in the center of the channel.

To analyze the voltage dependence of J_i, we must know the form of the dimensionless potential in the channel. We assume that the potential can be represented as the sum of the ion–channel interaction potential and a linear potential due to the applied transmembrane voltage:

$$\phi(x)=\phi^0(x)+\Delta\phi\frac{x}{\delta}. \tag{41}$$

Notice that if $\phi^0(x)=0$, $\phi(x)=0$ in the center of the channel. This is due to our reference convention. We had, in effect, assumed this superposition in writing eqn (31). The assumption of superposition implies that the applied transmembrane potential has a negligible effect on the interaction between the ion and the channel, i.e. the channel conformation $\phi^0(x)$ is independent of $\Delta\phi$. This is reasonable if we suppose that the dominant contribution to the ion–channel interaction potential is from chemical groups in the immediate neighborhood of the ion. The electric field strength in this neighborhood due to the ion will be much larger than the field strength due to the applied transmembrane potential and so will be the dominant force determining the conformational states of the neighboring chemical groups. For example, a rough estimate of the field strength at a distance of 10 Å from a unit point charge in a medium with a dielectric constant of 10 is 2×10^8 volts/meter. This is equivalent to a transmembrane voltage of one volt across a 50 Å membrane, roughly an order of magnitude larger than physiological transmembrane voltages. On the other hand, the experimental observation that the open probability of many channels is a function of voltage indicates that the above assumption is not strictly correct. Such observations can be considered as changes in $\phi^0(x)$ induced by changes in $\Delta\phi$. They are likely to be on a much longer time scale than transport through the channel and so we may still hope the assumption of superposition is reasonable. At any rate, the assumption of superposition is more convenient than rigorous.

The relationship between the intrinsic ion–channel interaction potential and the current–voltage relationship is a complicated one involving integrations over the potential profile in the channel. At extreme voltages this complicated relationship reduces to a much simpler relationship which depends only on the local properties of the potential profile at the ends of the channel. To intuit this idea, consider an ion entering the left end of the channel when the voltage is large and negative. Once the ion has moved a substantial distance into the channel it is overwhelmingly likely to be swept through to the other end due to the large electrical field. It therefore seems reasonable to expect that only those features of the potential near the left end of the channel would influence permeation. This intuitive idea is formalized in Appendix 1 through the use of an asymptotic analysis of the electrodiffusive resistance and the MFPTs. The essential conclusion of this appendix is that the potential and its slope at the ends of the channel are the dominant factors determining the current–voltage relationship at extreme voltages. In the other extreme for small field strengths, two cases exist. In the first case the ion–channel interaction potential is characterized by extreme variations in the potential compared to the thermal kinetic energy k_bT. In this case the characteristics of the potential at the tops of the barriers and bottoms of the wells are the dominant influences on permeation (Kramers, 1940; Cooper *et al.*, 1988a,b). In the second case the ion–channel interaction potential undergoes only modest variations relative to the mean thermal kinetic energy k_bT. In this case all features of the ion–channel interaction influence permeation. It is this last case that we consider in the body of this paper.

We have chosen five potential profiles which demonstrate these issues. Our starting place

is the classic constant field potential. Being the simplest possible form of the intrinsic ion–channel interaction potential, this profile emphasizes the dependence of the model on the concentration ratio. The next potential considered is the ramp potential (Fig. 3, panel 1). This potential has offsets at the ends of the channel and nonzero slopes but lacks any features at intervening points. The step potential (Fig. 3, panel 2) has offsets at the ends of the channel but zero slopes. This means that the change in the potential takes place suddenly rather than gradually as in the case of the ramp. The last potential of odd symmetry is the Z potential (Fig. 3, panel 3). The Z potential has no offsets but does have nonzero slopes and, like the step, undergoes a sudden change in the center of the channel. Finally, we consider single extremum potentials with even symmetry (Fig. 3, panel 4). The single extremum potentials are the even symmetry analogs of the Z potential, i.e. no offsets but nonzero slopes. The sudden transition in the middle of the channel is now in the slope instead of the potential.

These potential profiles introduce an additional parameter p into the calculations. Now the independence flux can be thought of as a function of the channel dimensions, diffusion coefficient, concentration (discussed in the previous section) and the three dimensionless variables u (1/2 the dimensionless potential difference), r (1/2 the logarithm of the concentration ratio) and p.

In light of our previous discussion about limiting behavior of the current–voltage relationship, we derive equations for two simple limits to the independence flux. First, we consider the flux near equilibrium (i.e. near the reversal potential). From eqn (38) we obtain:

$$-J_{\mathrm{iss}} \simeq \frac{n(-\delta/2)\,(\Delta\phi - \Delta\phi_{\mathrm{eq}})}{R_{\mathrm{c}}(r_n)} \tag{42}$$

where $R_{\mathrm{c}}(r_n)$ is the channel electrodiffusive resistance calculated at the value of $\Delta\phi$ that satisfies the Nernst equation. Thus R_{c} becomes a function of r_n.

In terms of the conventional conductance formalism, eqn (42) can be written:

$$I = G(\Delta V_{\mathrm{m}} - \Delta V_{\mathrm{eq}}) \tag{43}$$

$$G = \frac{z^2 \mathrm{e}^2 n(-\delta/2)}{k_{\mathrm{b}} T R_{\mathrm{c}}(r_n)} \tag{44}$$

with

$$\Delta V = \frac{z\mathrm{e}}{k_{\mathrm{b}} T}\,\Delta\phi.$$

We emphasize the fact that eqn (44) is not generally correct. Away from equilibrium the current–voltage relationship may be nonlinear. In this case the slope of the current voltage relationship cannot be used in eqn (43). For this reason the traditional definition of the conductance in eqn (43) is the chord conductance which in general depends on the applied voltage in addition to the parameters of eqn (44).

The other limit is that at extreme voltages. We do the asymptotic analysis for this case in Appendix 1. This analysis yields J_{i} in terms of $\phi^0(x)$ and its derivatives at the mouths of the channel.

$$-J_{\mathrm{i}} = \frac{AD}{\delta}\, n(\delta/2)\mathrm{e}^{-\phi^0(\delta/2)} \left(2u + \delta \frac{\mathrm{d}}{\mathrm{d}x}\,\phi^0(\delta/2) - \frac{\delta^2}{2u}\frac{\mathrm{d}^2}{\mathrm{d}x^2}\,\phi^0(\delta/2)\right) + O(1/u^2) \tag{45}$$

when $u \gg 0$ and:

$$\frac{AD}{\delta}\, n(-\delta/2)\mathrm{e}^{-\phi^0(-\delta/2)} \left(2u + \delta \frac{\mathrm{d}}{\mathrm{d}x}\,\phi^0(-\delta/2) - \frac{\delta^2}{2u}\frac{\mathrm{d}^2}{\mathrm{d}x^2}\,\phi^0(-\delta/2)\right) + O(1/u^2) \tag{46}$$

when $u \ll 0$. The notation $O(1/u^2)$ indicates that the remaining terms go to zero with order $1/u^2$ as $|u| \to \infty$. Let us now examine these expressions [eqns (42) through (46)] for the various potential functions described above.

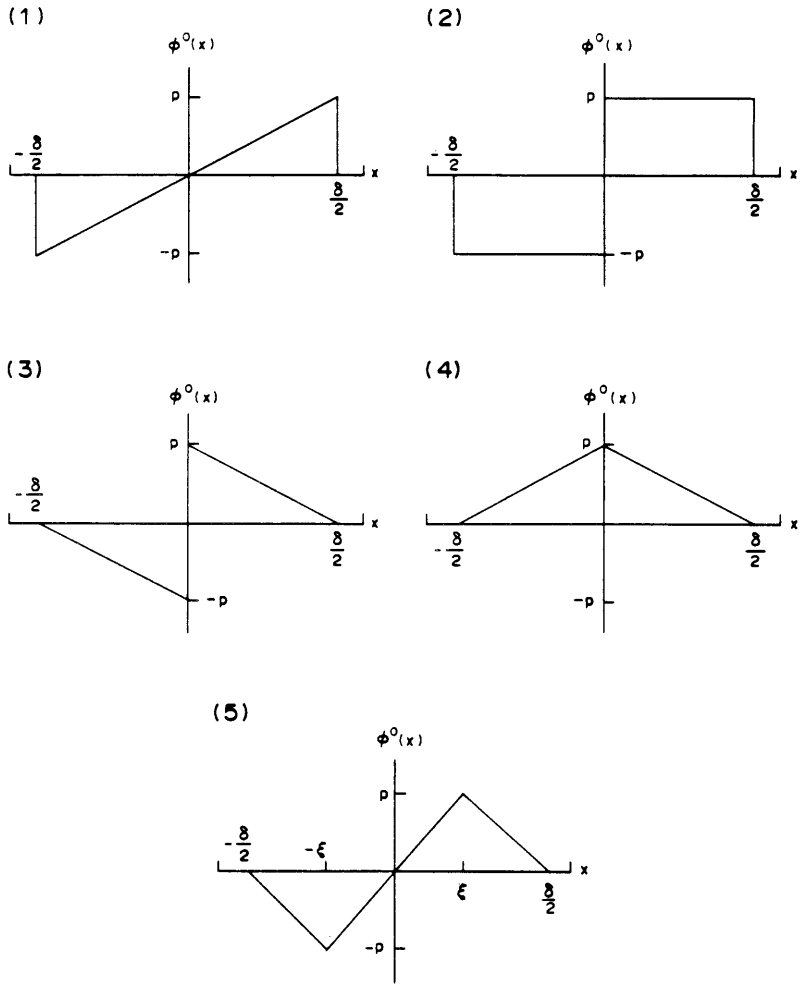

FIG. 3. Various ion–channel interaction potentials used in the model. Panel 1: ramp potential; panel 2: step potential; panel 3: Z potential; panel 4: single extremum potential; panel 5: double extrema potential.

(a) *Constant field potential*

In Fig. 4, we have plotted the constant field independence flux* holding the concentration on the left end of the channel fixed while varying the concentration on the right. A useful way of thinking about Fig. 4 is to consider each current–voltage relationship as a slice through a surface whose height is the current. This current depends on the concentration ratio (the coordinate axis coming out of the page) and the voltage. When the concentration ratio is zero $[n(\delta/2)=0]$ the current is always negative but asymptotically approaches zero at large positive voltages. When the concentration ratio becomes large $[n(\delta/2)\to\infty]$, the reversal potential goes to large negative voltages and the conductance at positive voltages becomes large. This dependence of the current–voltage relationship on the concentration ratio is the well known Goldman rectification (Goldman, 1943).

We now develop the details of the properties of the constant field independence flux. These results give some flavor of the expressions describing the current–voltage–concentration ratio surface. By evaluating R_c in eqn (40) for this simple form of $\phi^0(x)$ we obtain:

$$-J_i=\frac{DA2\bar{n}}{\delta}\left(\frac{u\sinh(u+r)}{\sinh(u)}\right). \tag{47}$$

*For easier comparison with real data, we plot currents instead of fluxes in all figures.

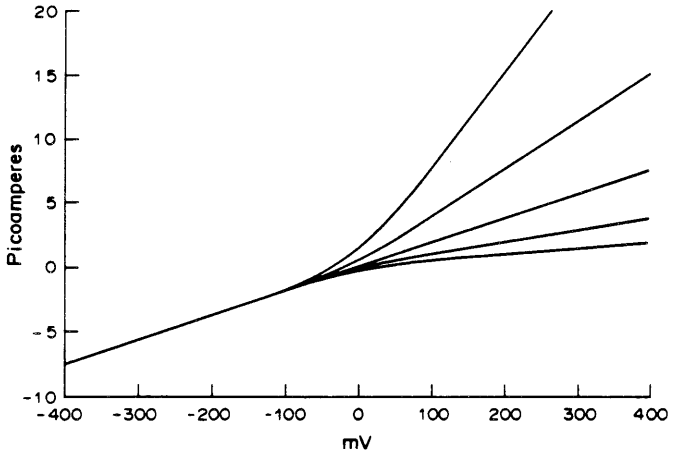

FIG. 4. Constant field flux without access effects as a function of the voltage and concentration ratio. Flux with ion–channel interaction potential identically zero. Channel length was set to 5 nm, channel radius 0.2 nm, and temperature 25°C as will be the case in all remaining plots. For this plot the channel diffusion coefficient was set at $0.1 \times 10^{-9} m^2/sec$ and concentration on the left side of the channel was fixed at 2 M (g_i 18.8 pS). Results were computed with negligible access effects. The concentration ratio 4, 2, 1, 1/2 and 1/4.

For future reference, we collect the equations for R_c for our entire set of potential profiles in Table 1. For the small signal (near equilibrium) conductance we have:

$$G_i = \begin{cases} g_i\left(\dfrac{\ln(r_n)}{1-1/r_n}\right), & r_n \neq 1 \\ g_i, & r_n = 1 \end{cases} \tag{48}$$

with

$$g_i = \frac{z^2 e^2 DA\bar{n}}{k_b T\delta}.$$

Notice that the ratio G_i/g_i can be written in terms of the hyperbolic sine as follows:

$$\frac{G_i}{g_i} = \frac{r}{\sinh(r)}. \tag{49}$$

This result is the same as the result for the constant field R_c if you substitute $-r$ for u everywhere in the expression in Table 1. This is a general result and thus we do not need a separate table for G_i. In symmetric concentrations and in the absence of access limitations, the constant field flux approaches the Ohmic limit. This can be seen by setting $r=0$ in eqn (47) to yield:

$$-J_{iss} = \frac{2}{\delta} DAnu. \tag{50}$$

Our other limit involves letting the transmembrane potential go to both positive and negative infinity in eqn (47). This yields:

$$\lim_{u\to\infty} -J_i = \frac{DAn(\delta/2)}{\delta} 2u \tag{51}$$

$$\lim_{u\to-\infty} -J_i = \frac{DAn(-\delta/2)}{\delta} 2u. \tag{52}$$

TABLE 1. INDEPENDENCE

	DAR_c/δ
Constant field	$\frac{\sinh(u)}{u}$
Ramp	$\frac{\sinh(u+p)}{u+p}$
Step	$\frac{\sinh(u+p)-\sinh(p)}{u}$
Z	$\frac{\sinh(u)-\sinh(p)}{u-p}$
Single extrema	$\frac{1}{2}\left[\frac{e^u}{u-p}-\frac{e^{-u}}{u+p}-e^p\left(\frac{1}{u-p}-\frac{1}{u+p}\right)\right]$

The various terms in the above expressions can be interpreted as follows. For all of the potentials of odd symmetry (constant field—Z) the slope can be factored out to yield expressions involving hyperbolic sines. In the case of an offset (ramp and step) the parameter p sums with the dimensionless applied voltage in the argument of first hyperbolic sine. In the case of a jump (step and Z) an additional hyperbolic sine with argument p is added. In the case of the single extremum potential the addition of an applied voltage breaks the symmetry of the potential and no convenient collection of terms is possible.

Consider the qualitative information we have in eqns (48) through (52). We know that the small signal conductance is a decreasing function of the concentration ratio. We also know that the asymptotic behavior of the current–voltage relationship is linear with slope proportional to concentration and intercept at the origin. Using this information and the reasonable expectation that the current–voltage relationship is smooth we could produce all of the qualitative features of Fig. 4. In particular, a knowledge of the asymptotic behavior provides enough information to obtain a rough approximation of the current–voltage relationship at voltages where the asymptotic results do not apply. This argument illustrates the utility of eqns (45) and (46). An important goal of this paper is to cultivate a qualitative understanding of the one-ion model that would allow the reader to make rough predictions about consequences of a particular feature of the ion–channel interaction potential on the current–voltage relationship.

Before proceeding we mention a simple result. If the constant field potential is offset by an amount p, the concentration is scaled by the Boltzmann factor of the offset. The result in this case is eqn (47) with the concentrations $n(-\delta/2)$ and $n(\delta/2)$ replaced by $n(-\delta/2)e^{-p}$ and $n(\delta/2)e^{-p}$. The small signal conductance and asymptotic results are similarly affected.

(b) *Ramp potential*

The ramp potential ($\phi^0(x)=px/\delta$) represents the simplest kind of odd symmetry. The potential energy of an ion in the channel varies smoothly from one end of the channel to the other. To understand the consequences of the ramp potential, consider the $J_i(u, r)$ surface normalized by the geometric average of the concentrations $\bar{n}$. The ramp potential causes a shift of the surface by $-p$ along the u (i.e. potential) axis and p along the r (i.e. concentration ratio) axis (Fig. 5). The ramp potential produces Goldman-like rectification with symmetric concentrations while producing an Ohmic current–voltage relationship when the concentration ratio is given by $r_n=e^{2p}$. This is analogous to Woodbury's (1971) finding that a channel with a sequence of linearly increasing barriers produces a linear current–voltage relationship when the logarithm of the concentration ratio is equal to the difference between the height of the first and last barriers.

Next consider the asymptotic properties of the independence flux. The ramp potential has an offset and a nonzero slope at either end of the channel. The effect of the offset is analogous

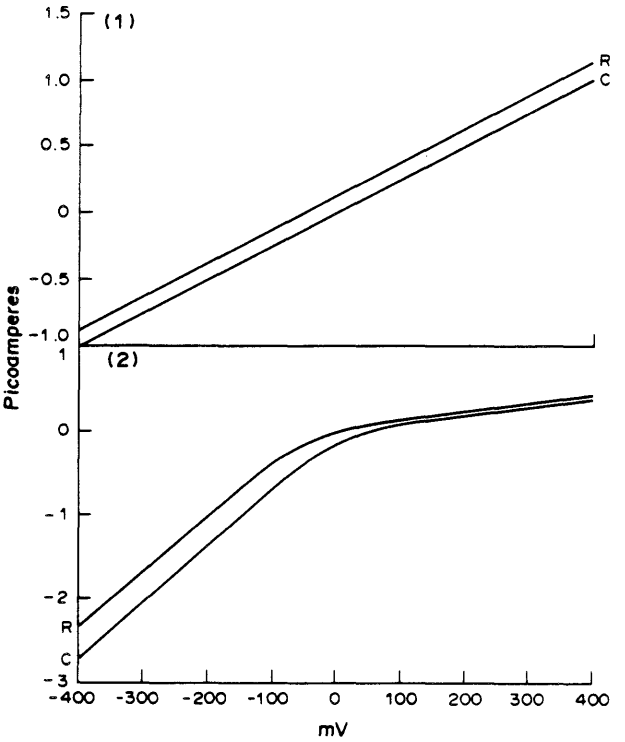

FIG. 5. Comparison of constant field and ramp potential independence fluxes without access effects. Flux with constant field and ramp potentials. The ramp potential has $p = 1k_bT$ and the diffusion constant is set to 0.01×10^{-9}m^2/sec for all remaining plots. Panel 1: $r_n = 1$ for constant field, $r_n = e^2$ for ramp; panel 2: $r_n = 1$ for ramp, $r_n = e^{-2}$ for constant field. R: ramp potential; C: constant field potential.

to the effect of the offset in the constant field potential except that the odd symmetry of the ramp produces offsets of opposite signs for the two ends of the channel. The slope produces a nonzero intercept of the linear asymptotes. If we set $r_n = e^{2p}$, the coefficients of eqns (45) and (46) will be equal and the asymptotic results will predict a shift of the current–voltage relationship by an amount proportional to the derivative of the potential at the ends of the channel. This gives precisely the shift by $-p$ discussed in the previous paragraph.

(c) *Step potential*

In the case of the ramp potential, the offsets at the ends of the channel came about through a steady increase in the potential as it traversed the channel. At the other extreme, the increase in the potential can be concentrated at a point as in the step potential ($\phi^0(x) = -p$ for $-\delta/2 \leq x \leq 0$ and $\phi^0(x) = p$ for $0 \leq x \leq \delta/2$).

Again we investigate the effect of the step potential on the normalized $J_i(u, r)$ surface by considering the small signal and asymptotic properties separately. At extreme voltages, the surface associated with the step potential will match the surface associated with the constant field potential by a shift of p along the r axis but, in contrast with the ramp potential, without a shift in the u axis (Fig. 6). In the small signal range, a shift in the r axis must be accompanied by a shift in the u axis of equal magnitude but of opposite sign because these are related by the Nernst potential. It is not true, however, that the ramp and the step potentials share the same tangents near equilibrium. In fact, for equivalent values of the parameters p, r and g_i, the ramp potential has the greater small signal conductance. Thus, a sudden change in the potential gives rise to a lower conductance than a gradual change in the potential.

(d) Z *potential*

The Z potential ($\phi^0(x) = 2px/\delta + p$ for $-\delta/2 < x < 0$ and $\phi^0(x) = 2px/\delta - p$ for $0 < x < \delta/2$) is

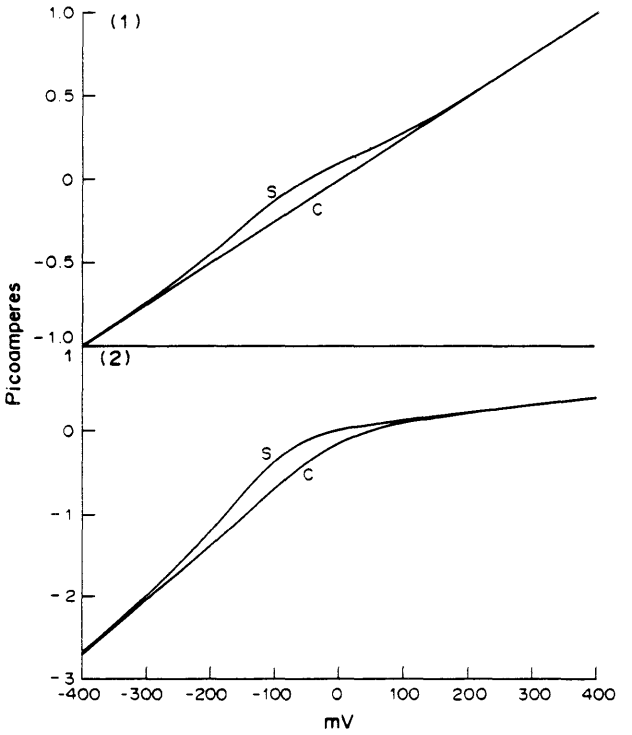

FIG. 6. Comparison of constant field and step potential independence fluxes without access effects. Flux with constant field and step potentials ($p = 1k_bT$), $r_n = 1$ for constant field potential and $r_n = e^2$ for the step potential. The step potential has the lower small signal conductance. S: step potential; C: constant field potential.

related to the step potential in the same way that the ramp potential is related to the constant field potential. Also the ramp and Z potentials are both limiting cases of a more general potential of odd symmetry having a well on the left end of the channel and a barrier on the right end (Fig. 3, panel 5). This profile is characterized by two parameters: p, the height (depth) of the barrier (well) and ξ, the distance of the barrier (well) from the center of the channel. With symmetric concentrations ($r = 0$), the small signal conductance becomes independent of the parameter ξ to yield:

$$G_i = g_i\left(\frac{p}{\sinh(p)}\right). \tag{53}$$

Thus, the $J_i(r, u)/\bar{n}$ surfaces associated with the ramp and Z potentials share the same tangent plane at $r = u = 0$. The Z potential has the feature that in symmetric concentrations, all of the rectification is due to the slope in the ion–channel interaction potential at the ends of the channel. Since the slope is the same at both ends of the channel, the asymptotic intercepts in symmetric concentrations will also be the same for both positive and negative voltages. This asymptotic intercept will be shifted an equal amount and in the opposite direction from the ramp potential for $r_n = e^2$ (compare Figs (9) and (11)). Thus, for both the step and Z, the jump in the potential results in a bulge in the current–voltage relationship near equilibrium (Fig. 7).

A useful exercise is to sketch both the ramp and the Z current–voltage relationships on the same plot for symmetric concentrations (see ramp potential in Fig. 5, panel 2, and Z potential in Fig. 7, panel 1). As mentioned above the relationships share the same tangent at equilibrium. Away from equilibrium the asymptotic results require that the two relationships diverge. These two curves define the limits of the family of curves produced when the parameter ξ of Fig. 3, panel 5 varies from 0 to $\delta/2$.

Let us summarize the sources of rectification for the potentials with odd symmetry. The first source is the classic Goldman rectification due to a difference in concentrations across

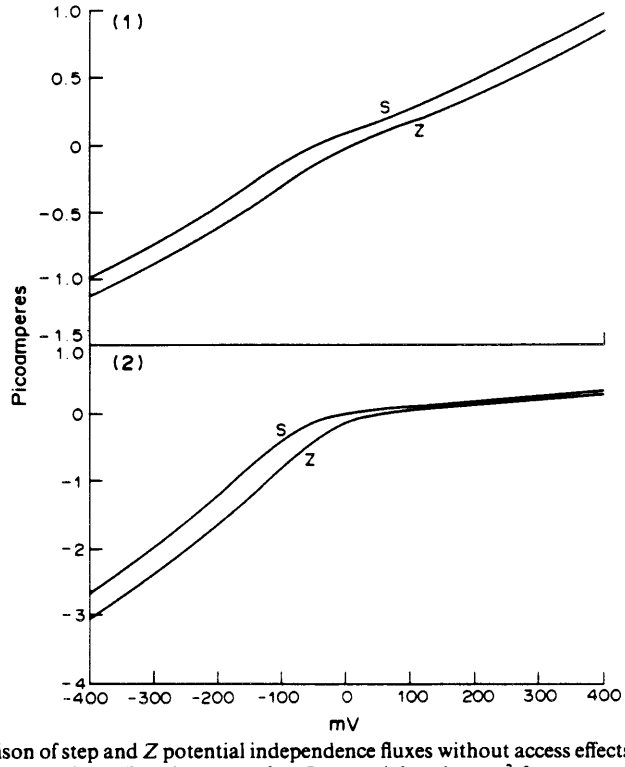

FIG. 7. Comparison of step and Z potential independence fluxes without access effects. Flux with step and Z potentials ($p = 1k_bT$). Panel 1: $r_n = 1$ for Z potential and $r_n = e^2$ for step potential; panel 2: $r_n = e^{-2}$ for Z potential and $r_n = 1$ for step potential. In this case notice that the fluxes are identical but shifted along the voltage axis proportional to the parameter $r = (1/2)\ln(r_n)$. S: step potential; Z: Z potential.

the channel. The second source is an offset in the potential at the ends of the channel. This causes the current–voltage relationship to appear qualitatively similar to Goldman rectification in the presence of symmetric concentrations. In both of these cases the straight line asymptotes have different slopes. The third source of rectification is a nonzero slope at the ends of the channel. This causes rectification near equilibrium in symmetric concentrations but not at extreme voltages. The asymptotic analysis demonstrates that this is due to a shift in the intercept of the asymptote. The odd potentials give rise to asymmetric current–voltage relationships when the baths have the same concentrations. In the next section we discuss potentials with even symmetry. These produce symmetric current–voltage curves in symmetric concentrations.

(e) *Single extremum potential*

We now consider a simple function which is even with respect to the center of the channel. The parameter p will specify the height of a barrier ($p > 0$) or the depth of a well ($p < 0$) that is centered in the channel (Fig. 3, panel 4). We designate this potential the single extremum potential ($\phi^0(x) = 2px/\delta + p$ for $-\delta/2 < x < 0$ and $\phi^0(x) = -2px/\delta + p$ for $0 < x < \delta/2$). Notice that the single extremum potential is the even symmetry analog to the Z potential. An important consequence of this is that the application of a transmembrane voltage results in symmetry breaking since the potential due to applied voltage is an odd function. This symmetry breaking causes a loss of symmetry in the equations for the model. As an example, Table 1 shows the electrodiffusive resistances of the five different potentials. The first term in each expression arises from the end points of the channel and thus involves u. In the case where there is an offset, these terms also include the parameter p. The second term in the step, Z, and single extremum potentials is due to the jump in potential in the center of the channel. The fact that constant field, ramp, step, and Z potentials have odd symmetry means that no symmetry breaking occurs when $\Delta\phi$ is added; thus, the denominator can be factored out and

one obtains expressions involving hyperbolic sines. In the case of the single extremum potential, no such factoring is possible.

For the symmetric barrier or well, there is no shift of the normalized flux surface on either the r or u axes because there is no offset at the ends of the channel (Fig. 8). Recall that at

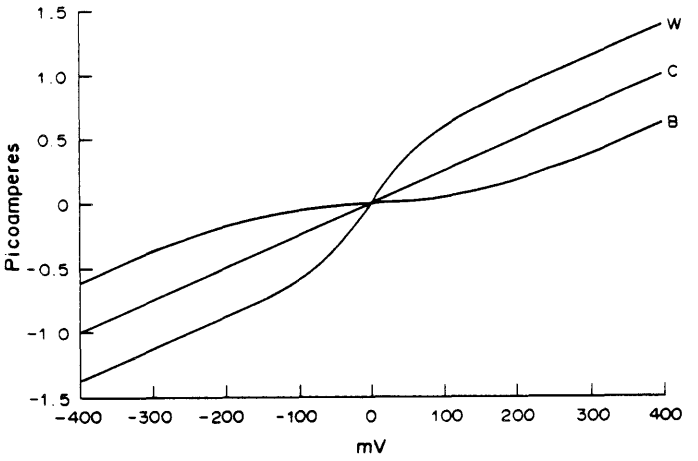

FIG. 8. Comparison of constant field, $3k_bT$ well and $3k_bT$ barrier independence fluxes without access effects. Concentrations are symmetric ($r_n = 1$) and equal to 2.64 M. Diffusion constant was set to 0.01×10^{-9}m^2/sec (g_i 2.5 pS). Notice that the well potential has a high slope conductance near equilibrium and asymptotically approaches the slope conductance of the constant field. Similarly, the barrier potential has a low slope conductance near equilibrium and asymptotically approaches the slope conductance of the constant field. W: well potential; C: constant field potential; B: barrier potential.

extreme voltages the slopes of the potential at the ends of the channel produce shifts in the intercepts of the straight line asymptotes. Since the single extremum potential is even with respect to the center of the channel, the slopes of the potential are equal in magnitude and opposite in sign at the two ends of the channel. This produces a rotation of the current–voltage relationship in the small signal range (as opposed to the bulge seen in the case of the Z potential). In the case of a well, the rotation is counter-clockwise producing an increase in the conductance relative to the constant field potential while in the case of the barrier the rotation is clockwise producing a decrease in the conductance.

2. *Independence Flux with Access Limitations*

We have now seen the behavior of the independence flux in the absence of access limitations. Let us see how access limitations change the shape of the current–voltage relationships. The qualitative effect is saturation of the flux with voltage. In all cases examined in the previous sections the asymptotic behavior of the flux was described by a straight line whose slope was determined by the offset and the concentration at the end of the channel. When access effects are included, the independence flux without access effects can be related to the independence flux with access effects through a dimensionless ratio of electrodiffusive resistances:

$$J_{ia} = \frac{J_i R_c}{R_l + R_c + R_r} = J_i R. \tag{54}$$

We can combine eqn (54) with eqn (A3) of Appendix 1 to obtain the asymptotic behavior of this resistance ratio. From this we can show that the flux saturates to a fixed value determined by the voltage independent rate at which ions encounter the channel:

$$\lim_{u \to \infty} -J_{ia} = \frac{n(\infty)}{R_r} \tag{55}$$

$$\lim_{u \to -\infty} J_{ia} = \frac{n(-\infty)}{R_l}. \tag{56}$$

At large voltages, the resistance ratio asymptotically approaches a hyperbolic rate of saturation with half saturation value given by:

$$\Delta\phi_{1/2} = \frac{\delta e^{\phi^0(\delta/2)}}{ADR_r}, \quad \text{as } \Delta\phi \to \infty \tag{57}$$

$$\Delta\phi_{1/2} = \frac{\delta e^{\phi^0(-\delta/2)}}{ADR_l}, \quad \text{as } \Delta\phi \to -\infty. \tag{58}$$

In Fig. 9, we plot the currents and their associated resistance ratios for the constant field, the

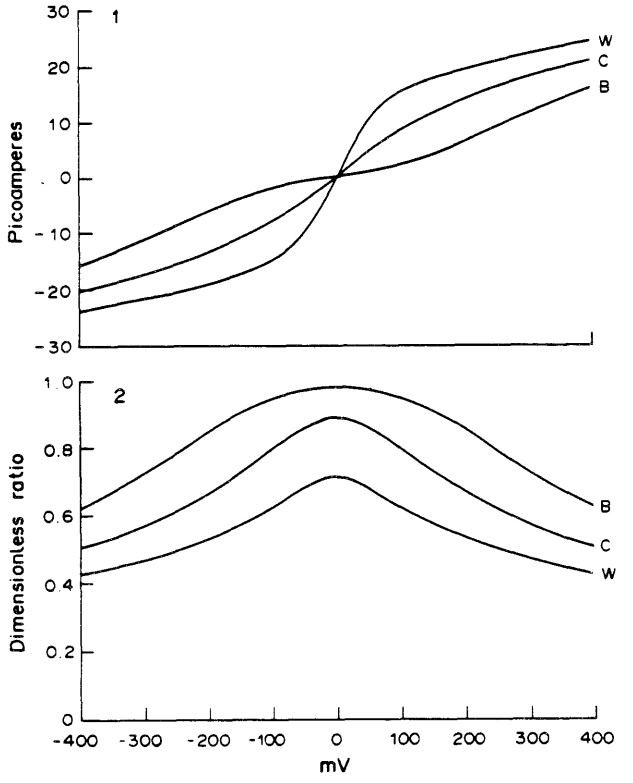

FIG. 9. Comparison of constant field, $3k_bT$ well and $3k_bT$ barrier independence fluxes with access effects. Panel 1: fluxes analogous to those of Fig. 8 but with the diffusion coefficient set at 1.5×10^{-9}m^2/sec and with $4k_bT$ access barriers; panel 2: electrodiffusive resistance ratio for fluxes of panel 1.

barrier and the well potentials. The saturation of flux with voltage is evident in all three cases (compare with Fig. (8)).

Access resistance effects are important when the bath resistances become comparable to the channel resistance. The bath resistance can become large for several reasons. The simplest has to do with the process of an ion finding the mouth of the channel. As an ion approaches the channel from a distance, the cross-sectional area decreases as r^2. This is analogous to an electrical convergence resistance. In Fig. 10 we have polotted the constant field potential and included the effect of the r^2 dependence of the cross-sectional area. Thus the process of an ion gaining access to the mouth of a channel gives rise to an entropic barrier in the potential. Another obvious source of such a barrier to entry is the process of ion dehydration.

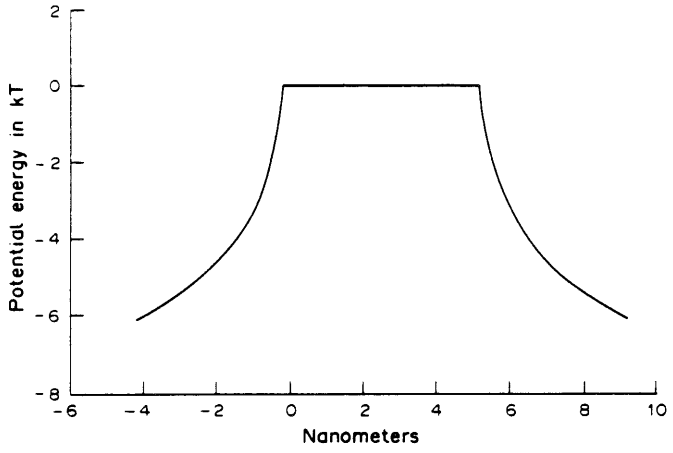

FIG. 10. Constant field potential including effect of r^2 dependence of cross sectional area of bath. This plot demonstrates the effect of redefining the dimensionless potential to include the position dependence of the cross sectional area of the bath, i.e. $\phi'(r)=\phi(r)+\ln[A(r)/A(0)]$. The intrinsic ion–channel interaction potential is the constant field.

IV. SATURATION FLUX (J_s)

In Section III we demonstrated that, for a fixed voltage, the effect of varying the magnitude of the concentration vector was to give rise to a flux with hyperbolic saturation. This saturation was completely characterized by a maximum value of the flux (eqn (35)) and a concentration at which the current is half of its maximum value (eqn (36)), each a function of the voltage. Here we discuss the saturation flux.

As in the last section, we begin by making the assumption of negligible access resistances. If we factor out the geometric average of the concentrations from both the numerator and denominator of eqn (23), take the limit as the average goes to infinity, let R_l and R_r become negligible with respect to R_c, and rewrite the result in terms of u and r, we obtain:

$$-J_s=\frac{2\sinh(u+r)}{\tau_r e^{u+r}+\tau_l e^{-u-r}}. \tag{59}$$

Several general features of eqn (59) as compared to eqn (40) for the independence flux are worth noting. The independence flux depends on the geometric average of the concentrations. For the saturation flux, this dependence was eliminated by taking the large concentration limit. Notice also that the saturation flux does not depend on the channel cross sectional area as does the independence flux.

Another important difference between the independence flux and the saturation flux is that the saturation flux depends on MFPTs and the independence flux does not. The dependence of eqn (59) on the MFPTs allows us to obtain some insight into the role of MFPTs in the one-ion model. Note that if the concentration on the right side of the channel is set to zero ($r\to-\infty$), the saturation flux is equal to $1/\tau_l$. Hence, the mean first passage times represent the maximum flux through a one-ion channel in the so called zero trans case (Jakobsson and Chiu, 1987). At saturation, whenever an ion exits the channel, it is immediately replaced by another ion and transport is limited by the rate at which the channel can process an ion. In the steady state, this rate is related to the reciprocal of the mean passage time of an ion through the channel.

We now derive the small and large voltage limits of eqn (59). In the small signal range, the sum of u and r is small and the exponentials in the denominator of eqn (59) are approximately one. The sum of the two passage times then simplifies to the product of two integrals and eqn (59) becomes:

$$-J_s=\frac{4D}{\delta^2}(u+r)\left[\int_{-1}^{1}e^{\phi(\delta\xi/2)}\,d\xi\int_{-1}^{1}e^{-\phi(\delta\xi/2)}\,d\xi\right]^{-1}. \tag{60}$$

From this we can obtain an expression for the small signal conductance:

$$G = \frac{4z^2e^2D}{k_bT\delta^2}\left[\int_{-1}^{1} e^{\phi(\delta\xi/2)}\,d\xi \int_{-1}^{1} e^{-\phi(\delta\xi/2)}\,d\xi\right]^{-1}. \tag{61}$$

In evaluating the integrals of eqns (60) and (61), we can make use of the fact that in the small signal range the potential is approximately equal to the equilibrium potential and hence from the Nernst equation $u \cong -r$.

In Appendix 1 we show that the large voltage limit of eqn (59) is:

$$-J_s = \frac{D}{\delta^2}\left[2u - \beta_p + \frac{1}{2u}(\beta_p^2 - \gamma_p)\right] + O(1/u^2),\ u \gg 0 \tag{62}$$

$$-J_s = \frac{D}{\delta^2}\left[2u - \beta_n + \frac{1}{2u}(\beta_n^2 - \gamma_n)\right] + O(1/u^2),\ u \ll 0. \tag{63}$$

The expressions for the βs and the γs are lengthy and will not be repeated here (see Appendix 1, eqns (A35) and (A36) for details). The point we want to make here is that the βs are functions of the values of the ion–channel interaction potential at the ends of the channel while the γs are functions of the derivatives of the ion–channel interaction potential at the ends of the channel. The asymptotic results demonstrate that the limiting slope of the saturation flux depends only on the channel length and diffusion constant and not on any feature of the intrinsic ion–channel interaction potential. The limiting slope of these equations is simply D/δ^2.

The following argument shows why one might expect the limiting slope of the saturation flux to be independent of the intrinsic ion–channel interaction potential. The saturation flux, through its dependence on the passage times, involves two integrations of the exponential of the potential profile in the channel while the independence flux involves only one. Consequently, at extreme voltages, features of the model which determined the asymptotic slope of the independence flux effect the asymptotic intercept of the saturation flux (see Appendix 1). This means that the limiting slope of the saturation flux is independent of the features of the ion–channel interaction potential.

1. *Constant Field Potential*

We proceed, as in the case of the independence flux, by presenting the constant field results in detail. This will be followed by a qualitative description of the saturation flux for the other potential profiles we have been using. We summarize the quantitative results for all the potential profiles in Table 2. As was the case with the independence flux, the constant field potential provides an opportunity to obtain manageable results which still have many of the important features of the general one-ion model. In particular, interesting similarities between the saturation flux, MFPTs, and the problem of random walks are most apparent for the constant field case. The constant field saturation flux also has the unique property that a series expansion exists which converges for all nonzero values of the voltage. This series is of the same form as the asymptotic expansions obtained in Appendix 1 which in general converge only at extreme voltages. Finally, the constant field saturation flux illustrates an important general characteristic of the one-ion model, the current–voltage relationship tends to become more linear with increasing concentration.

Using the constant field potential in eqn (59) yields the following result:

$$-J_s = \frac{2uD}{\delta^2}\left(\frac{u\sinh(u+r)}{u\sinh(u+r) - \sinh(u)\sinh(r)}\right). \tag{64}$$

In the symmetric case, $n(\delta/2) = n(-\delta/2)$ $(r=0)$, eqn (60), like the independence flux reduces to an Ohmic limit:

$$-J_s = \frac{2D}{\delta^2}u. \tag{65}$$

TABLE 2. SATURATION

	$\frac{D}{\delta^2}(\tau_r e^{u+r}+\tau_l e^{-(u+r)})$
Constant field	$\frac{1}{2u^2}[\cosh(u-r)-\cosh(u+r)+2u\sinh(u+r)]$
Ramp	$\frac{1}{2(u+p)^2}[\cosh(u-r+2p)-\cosh(u+r)+2(u+p)\sinh(u+r)]$
Step	$\frac{1}{2u^2}[\cosh(u-r+2p)-\cosh(u+r)+2u\sinh(u+r)+\sinh(p)\{4\sinh(r-p)-2\sinh(u+r-p)\}]$
Z	$\frac{1}{2(u-p)^2}[\cosh(u-r)-\cosh(u+r)+2(u-p)\sinh(u+r)+\sinh(p)\{4\sinh(r)-2\sinh(u+r-p)\}]$
Single extremum	$\frac{1}{2(u^2-p^2)}\left[\cosh(u-r)-\frac{u^2+p^2}{u^2-p^2}\cosh(u+r)+2u\sinh(u+r)-\frac{4p}{u^2-p^2}\{u\sinh(p)\sinh(r)+p\cosh(p)\cosh(r)\}\right]$

We have collected corresponding terms from the right and left passage times and so the leading two terms, having the same sign, are hyperbolic cosines. When offsets are added (ramp and step) at the ends of the channel the parameter p appears in the argument of the first hyperbolic cosine. The influence of the slopes at ends of the channel (ramp, Z and single extremum) appear in the denominators and in the coefficient of the third term for the ramp and the Z potentials. The analogous term in the single extremum potential cancels with terms in the denominator. Finally, structural features inside the channel such as jumps in the potential (step and Z) or extrema (single extremum) produce additional terms.

This expression tells us that for a $1k_bT$ difference in potential energy across the membrane, the average time required for the net movement of one ion through the channel at saturation is given by:

$$t=\frac{\delta^2}{D}. \tag{66}$$

This result agrees, within a factor of two, with two other results derived from different boundary conditions. These are the MFPT in the absence of a field [eqns (20) and (21) with $\phi(x)\equiv 0$]:

$$\tau=\frac{\delta^2}{2D} \tag{67}$$

and the Einstein (1926) relationship for the average squared distance travelled by a random walker in a time t:

$$\langle x^2\rangle=2Dt. \tag{68}$$

This idea of a transport time per k_bT of driving force is closely related to the small signal conductance under saturating conditions. For the general expression we have:

$$G_s=\begin{cases} g_s\,\dfrac{r}{\sinh(r)}, & r\neq 0 \\ g_s, & r=0 \end{cases} \tag{69}$$

with

$$g_s=\frac{I}{V}=\left(\frac{ze}{k_bT}\right)\left(\frac{zeD}{\delta^2}\right).$$

Here we see that g_s, the conductance in the Ohmic limit, is proportional to the reciprocal of this normalized transport time.

The constant field result [eqn (64)] can also be expressed as a power series in $1/u$ emphasizing the dependence of the saturation flux on the concentration ratio at extreme voltages:

$$-J_s = \frac{2uD}{\delta^2} \sum_{k=0}^{\infty} \left(\frac{1}{u}\right)^k \left(\frac{\sinh(u)\sinh(r)}{\sinh(u+r)}\right)^k, \quad u \neq 0. \tag{70}$$

In the limit of extreme voltages the first few terms of eqn (70) dominate and the coefficients of the powers of $1/u$ depend only on r:

$$-J = \frac{D}{\delta^2}\left[2u + 2e^{-r}\sinh(r) + \frac{2}{u}\left(e^{-r}\sinh(r)\right)^2\right] + O(1/u^2), \quad u \gg 0 \tag{71}$$

$$-J = \frac{D}{\delta^2}\left[2u + 2e^{r}\sinh(r) + \frac{2}{u}\left(e^{r}\sinh(r)\right)^2\right] + O(1/u^2), \quad u \ll 0. \tag{72}$$

When the concentrations are unequal, the voltage dependence of the saturation and independence fluxes are seen to be quite different (see Figs 4 and 11). Near equilibrium the

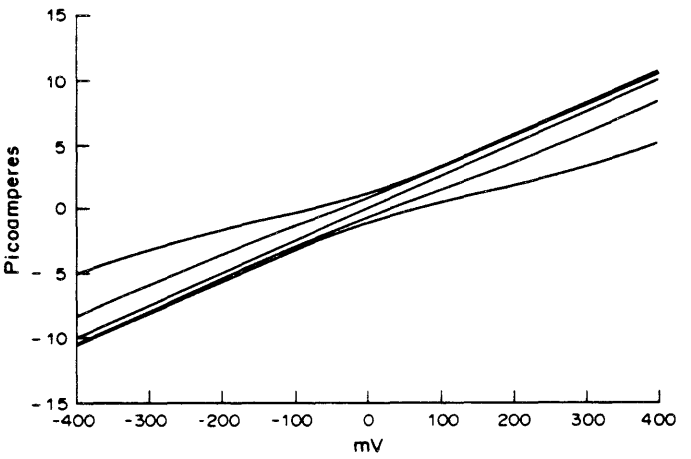

FIG. 11. The constant field saturation flux as a function of voltage and concentration ratio. Fluxes analogous to those of Fig. 4 except under conditions where the channel is always occupied. $r_n = 1/16, 1/4, 1, 4, 16$. Remaining parameters are the same as Fig. 4. g_s 25 pS.

current–voltage relationship rectifies in a qualitatively similar way to the independence flux, but to a lesser degree. This linearization of the constant field saturation flux under asymmetric conditions relative to the independence flux is a general feature of the one-ion channel model and is due to the asymptotic approach to a slope equal to the symmetric ($r = 0$) case.

2. *Potentials with Odd Symmetry*

As was the case with the independence flux, the ramp potential gives rise to a shift of the current–voltage–concentration ratio surface by $-p$ along the u axis and p along the r axis. Consequently, the ramp potential produces rectification in the saturation flux in symmetric concentrations in a way that is completely analogous to the rectification due to asymmetric concentrations in the constant field case. From this it follows that when the concentrations are such that $\Delta\phi_{eq} = \phi^0(-\delta/2) - \phi^0(\delta/2) \equiv -\Delta\phi^0$, we obtain the conductance of the constant field channel under symmetric conditions.

Two observations are useful for providing insight into the properties of the saturation flux in the case of the step potential. If the parameter r is set equal to the parameter p, the form of

the constant field saturation flux is recovered (see Table 2). Physically this is equivalent to setting the concentration ratio such that the concentration just inside the left end of the channel is kept equal to the concentration just inside the right end of the channel. The result is a $J_s(u, r=p, p)$ surface which is equivalent to the $J_s(u, r, p=0)$ surface. The second observation is that in symmetric concentrations the step potential saturation flux no longer rectifies (see Fig. 12). Two competing effects cause this disappearance of rectification. When

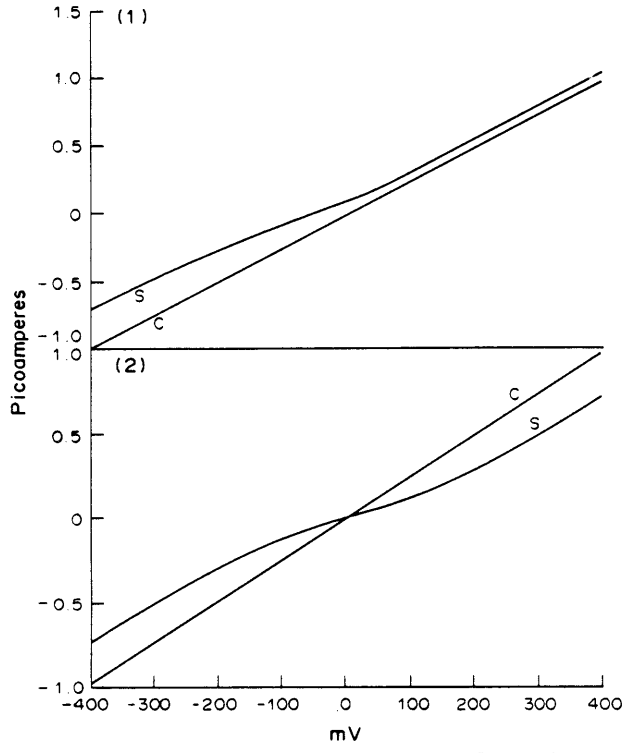

FIG. 12. Comparison of constant field and step potential saturation fluxes. Fluxes analogous to those of Fig. 6 except under conditions where the channel is always occupied by an ion. Panel 1: $r_n = 1$ for the constant field potential and $r_n = e^2$ for the step potential; panel 2: $r_n = 1$ for both the constant field and the step potentials. Flux for the Z potential flux can be obtained by shifting the step potential flux along voltage axis as can the ramp potential flux from the constant field potential flux.

the concentrations are equal on both ends of the channel, the channel is much more likely to be occupied by an ion entering the low potential end. In contrast, an ion having entered the high potential end is more likely to traverse the channel than an ion entering from the low potential end. This argument also holds for the ramp potential and accounts for the linearization of the current–voltage relationship.

As already noted in the discussion of the independence flux, the relationship between the Z potential and the step potential is analogous to the relationship between the constant field potential and the ramp potential. The saturation flux for the Z potential, with $r_n = 1$, is identical to that of the step potential, with $r_n = e^2$ except that the flux for the Z potential must be shifted so that it goes through the origin (see Fig. 12). This connection leads to another conclusion. Recall that the Z potential independence flux was weakly rectifying due to the effect of the slope of the potential at the ends of the channel. Also note that a jump has no consequence in the asymptotic behavior of the independence flux (see Appendix 1). We argued above that the jump in the step potential resulted in a complete loss of rectification in the limit of saturating concentrations. In the case of the Z potential, the rectification due to the jump in the limit of saturating concentrations overwhelms the effect of the slope of the potential and the rectification changes from inward at low concentrations to outward at high concentrations. We will return to this issue in the next section when we discuss the voltage dependence of the half saturation concentration.

3. *Single Extremum Potential*

The observations made above for the potentials with odd symmetry have somewhat different consequences for the single extremum potential. The symmetry breaking of the combination of the odd symmetry of the applied potential with the even symmetry of the ion–channel interaction potential leads in general to more complicated results. This is particularly true of the small signal conductance. As was the case in the analysis of the odd potential functions, insights can be obtained with the appropriate choice of the parameter r. The expressions involving the single extremum potential, being of even symmetry, would be expected to simplify in the case of symmetric concentrations, i.e. $r=0$. This simplification is most striking for the small signal conductance and we have:

$$G_s = g_s \left(\frac{p}{2 \sinh(p/2)} \right)^2 . \tag{73}$$

Notice, that if we define $p' = p/2$, the dependence of the small signal conductance on p' is the same as the dependence of the small signal conductance on r in the constant field case. This is analogous to the relationship between the constant field and the step potential small signal conductances when $r=p$. Also notice that, as was the case for the step potential, the result is independent of the sign of p. This last point leads to the realization that while the well and barrier have opposite effects on the small signal conductance of the independence flux, they have the same effect on the small signal conductance of the saturation flux (see Fig. 13). This

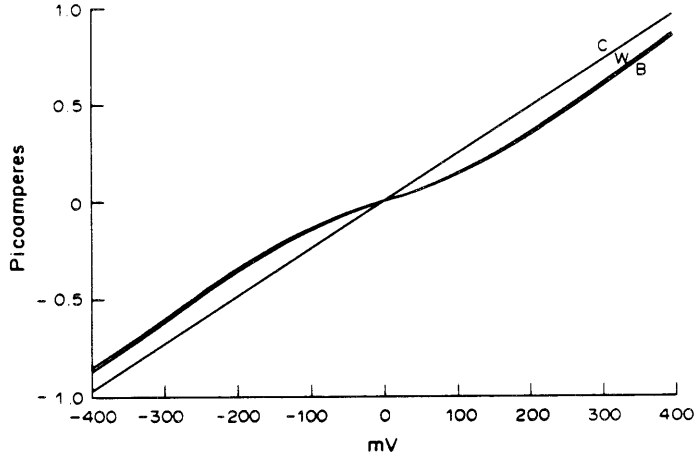

FIG. 13. Comparison of constant field, $3k_bT$ well and $3k_bT$ barrier saturation fluxes. Fluxes analogous to those of Fig. 8 except under conditions where the channel is always occupied by an ion. Remaining parameters are the same as Fig. 8.

implies that in the case of the well, there must be a transition analogous to the transition that occurred with the Z potential. Due to the even symmetry of the well, the transition is in the concavity of the current–voltage relationship rather than a transition from sub- to superlinearity in the current–voltage relationship. Inspection of Fig. 13 also reveals that in the small signal range under saturating conditions, both a barrier and a well result in a decrease in the channel conductance (increase in channel transport time). This observation suggests the stronger result (which we prove in Appendix 2) that the constant field potential has the maximum possible small signal conductance under saturating conditions.

The consequences of access effects on the saturation flux are more subtle than was the case for the independence flux. With the saturation flux we have, by assumption, precluded the possibility of access limitations. In taking the high concentration limit, we have implicitly assumed that the baths on either side of the channel can always supply ions to the channel at a rate that is much greater than the rate at which ions exit. One way of rationalizing this is to say that we are only considering voltages at which this assumption remains true. This

suggests that the asymptotic dependence of the saturation flux with voltage is not physically realizable. Disregarding this issue for the moment, the formal consequence of neglecting access effects in the high concentration limit of eqn (23) is the loss of reentrance effects on the occupancy time. Again we are confronted with a logical inconsistency since at infinite concentrations one might argue that no reentrances could occur. This inconsistency is more worrisome on mathematical grounds than physical grounds. The point we make here is that the saturation flux is a construct of conceptual use rather than a physically realizable feature of the model. We will return to these issues in the discussion section where we consider the general validity of the one-ion model.

V. HALF SATURATION CONCENTRATION ($n_{1/2}$)

The remaining piece of information needed to completely characterize the current–voltage–concentration surface is the rate of saturation of the flux with increasing concentration. In complete analogy with Michaelis–Menten enzyme kinetics, this rate of saturation is characterized by a single parameter, the substrate concentration which leads to half maximal catalytic velocity. In this formulation, we have not set the product concentration to zero (as is done in enzyme kinetics) and so the concentration of ions is a vector quantity. If we fix the ratio of the concentrations at the ends of the channel and fix the transmembrane voltage, we will obtain a right rectangular hyperbolic dependence of the flux on the geometric average of the concentrations. Hence, the functional dependence of the saturation flux and the half saturation concentration on the parameters u, r and p is sufficient to specify the one-ion model for the potentials considered here.

In the presentation of the half saturation concentration, we will develop two conceptual approaches. The first approach relates the half saturation concentration to the ratio of the saturation flux and the independence flux. This will allow convenient construction of expressions for the half saturation concentration by taking ratios of the entries of Tables 1 and 2. The second approach relates the channel affinities to the half saturation concentration and so makes the connection with more traditional methods in enzyme kinetics. We will also present a qualitative discussion of the five potential profiles paralleling what was done with the independence and saturation fluxes.

1. *Negligible Access Effects*

As in the case of the independence and saturation fluxes, we assume negligible access resistances. In the final section we modify our results to account for access limitations. From eqns (35) and (37) we can obtain an expression for the half saturation concentration as follows:

$$\bar{n}_{1/2} = \frac{J_s}{J_i}\bar{n}. \tag{74}$$

Combining eqn (74) with eqn (40) for the independence flux and eqn (59) for the saturation flux, we have:

$$\bar{n}_{1/2} = \frac{R_c}{\tau_r e^{u+r} + \tau_l e^{-u-r}}. \tag{75}$$

Equation (74) is general if reentrances are included while eqn (75) assumes that only one permeant species is present and access effects are negligible. We can also cast the channel affinity in terms of the components due to ions entering from the left and right ends of the channel respectively. From eqn (75) we have:

$$K_{al} = \frac{\tau_l e^{-u}}{R_c} \tag{76}$$

$$K_{ar} = \frac{\tau_r e^{u}}{R_c}. \tag{77}$$

The left and right affinity constants can be directly measured in a zero trans experiment. In

the zero trans case the geometric average of the left and right concentrations is zero and so we must consider the asymmetric half saturation concentrations. These are obtained by multiplying by e^{r} and e^{-r} and we have:

$$n(-\delta/2)_{1/2} = \frac{1}{K_{al}}, \quad \text{for } n(\delta/2)=0 \tag{78}$$

$$n(\delta/2)_{1/2} = \frac{1}{K_{ar}}, \quad \text{for } n(-\delta/2)=0. \tag{79}$$

Hence, by measuring the current–voltage relationship at several concentrations, with the opposite concentration set to zero, K_{al} and K_{ar} can be measured. From this, the voltage and concentration dependence of the empty probability can be determined. With these definitions we shall again consider several specific forms of the ion–channel interaction potential.

For the channel occupancy, the assumption of negligible access effects is equivalent to setting the concentrations at the ends of the channel to their equilibrium values (Levitt, 1986). This is the same as assuming that the rate at which ions are transported through the channel is small compared to the rapid exchange of ions between the bath and the channel mouth. The asymptotic results of the previous two sections indicate that at extreme voltages the channel flux increases linearly with the voltage. It follows that the assumption of negligible access affects must break down at large voltages. This results in a somewhat nonintuitive expression for the asymptotic behavior of the half saturation concentration. From Appendix 1 we have:

$$\bar{n}_{1/2} = \frac{1}{\delta A\sqrt{r_n}} e^{\phi^0(\delta/2)}\left[1 - \frac{1}{2u}(\delta\phi^{0\prime}(\delta/2)+\beta_p)\right] + O(1/u^2) \tag{80}$$

when $u \gg 0$ and:

$$\bar{n}_{1/2} \simeq \frac{\sqrt{r_n}}{\delta A} e^{\phi^0(-\delta/2)}\left[1 - \frac{1}{2u}(\delta\phi^{0\prime}(-\delta/2)+\beta_n)\right] + O(1/u^2) \tag{81}$$

when $u \ll 0$. Here, we use the prime to indicate the first derivative. Notice that the limiting value of the half saturation concentration is independent of the voltage and is determined by the Boltzmann factor at the end of the channel into which ions are being drawn by the applied voltage. This is a direct consequence of the assumption of negligible access limitations. The rate of approach to this limiting value depends on the difference between the intercepts of the linear asymptotes of the saturation and independence fluxes. This reflects the dependence of the half saturation concentration on both the passage times and the electrodiffusive resistance. We can also make use of the Boltzmann distribution to obtain a relatively simple expression for the half saturation concentration at equilibrium:

$$\bar{n}_{1/2} = \left[A\int_o^\delta e^{-\phi(x)}dx\right]^{-1}. \tag{82}$$

The general expressions for the half saturation concentration for the various potential profiles can be obtained from Tables 1 and 2 and eqn (74). As in the case of the independence and saturation fluxes, we consider the general expressions for the constant field case. For the remaining cases, we will emphasize the asymptotic and equilibrium expressions.

(a) *Constant field potential*

For the constant field potential, eqn (75) is:

$$\bar{n}_{1/2} = \frac{1}{A\delta}\left(\frac{u\sinh(u)}{u\sinh(u+r) - 2\sinh(u)\sinh(r)}\right). \tag{83}$$

Notice that with symmetric concentrations, the half saturation concentration is the reciprocal of the volume of the channel. We emphasize that this is the volume available to the center of the ion and not the total volume of the channel. Thus, the channel is occupied one half of the time when the concentration outside the channel is equal to twice the effective concentration inside the channel. In terms of the left and right affinities:

$$K_{al} = \frac{A\delta}{2}\left(\frac{\sinh(u) - u[\cosh(u) - \sinh(u)]}{u\sinh(u)}\right) \tag{84}$$

$$K_{ar} = -\frac{A\delta}{2}\left(\frac{\sinh(u) - u[\cosh(u) + \sinh(u)]}{u\sinh(u)}\right). \tag{85}$$

The qualitative properties of the empty probability with the constant field potential can be understood by considering the behavior of the affinities as a function of voltage. To begin with, notice that $K_{al} + K_{ar} = A\delta$. The consequence of this is that with $\Delta\phi = -\infty$, the channel binds ions with the same affinity as it would with zero transmembrane voltage and the concentrations in both baths equal to the concentration in the left bath. Similarly with $\Delta\phi = \infty$, the occupancy of the channel behaves as if it were at zero transmembrane voltage with both concentrations equal to the concentration in the right bath. Finally when $\Delta\phi = 0$, the channel is occupied as if it were at zero transmembrane voltage and the concentration was the arithmetic average of the concentrations in the right and left baths.

Alternatively, we can consider the dependence of the half saturation concentration on the concentration ratio. The rate at which the current approaches the saturation value is more rapid when the applied transmembrane voltage draws ions in from the side of the channel with the higher concentration. This is a result of the fact that at large applied voltages the channel occupancy is dominated by ions which enter from the side of the channel that is at the higher potential. To better understand this phenomena, we consider the concentration profile in the channel, the integral of which is the channel occupancy.

By assumption, the concentrations at the boundaries are held fixed at their equilibrium value. If we consider the left boundary, the concentration at a point in the channel will approach the concentration at the left boundary when negative voltages are applied. The rate of approach to the boundary concentration depends on the distance from the boundary and the nature of the potential at intervening points. In the case of the constant field potential, the concentration profile in the absence of an applied voltage is a linear function of position. When a voltage is applied, the contribution to the concentration at a point due to ions entering from the high potential end of the channel increases and the contribution due to ions entering from the low potential end of the channel decreases (see Fig. 14). Thus in asymmetric concentrations, the channel will saturate more quickly when a voltage is applied that draws ions in from the high concentration side verses the low concentration side.

The ability of the one-ion model to saturate is the mechanism by which the current–voltage relationship tends to become more linear with increasing concentration (compare Figs 4 and 11). In particular, as discussed above, this saturation is asymmetric for asymmetric potentials and the polarity of the asymmetry is opposite to the polarity of the asymmetry of the independence flux. In the constant field case when driving curent from the high concentration end of the channel, the current will be further up the saturation curve compared with the current under a similar driving force in the opposite direction. If we fix the concentration ratio and vary the geometric average of the concentration, at low concentrations where the independence flux is a good approximation, the current will rectify according to Goldman. As the geometric average of the concentration is increased, the current driven from the high concentration side will saturate more quickly than current driven from the low concentration side.

As in the case of the indpendence flux, the effect of an offset on the constant field result can be obtained by replacing the concentrations with the concentrations scaled by the Boltzmann factor e^{-p}. The consequence of this is that the effective volume of the channel changes and we replace $A\delta$ of the constant field result [eqns (83) through (85)] with $A\delta e^{-p}$.

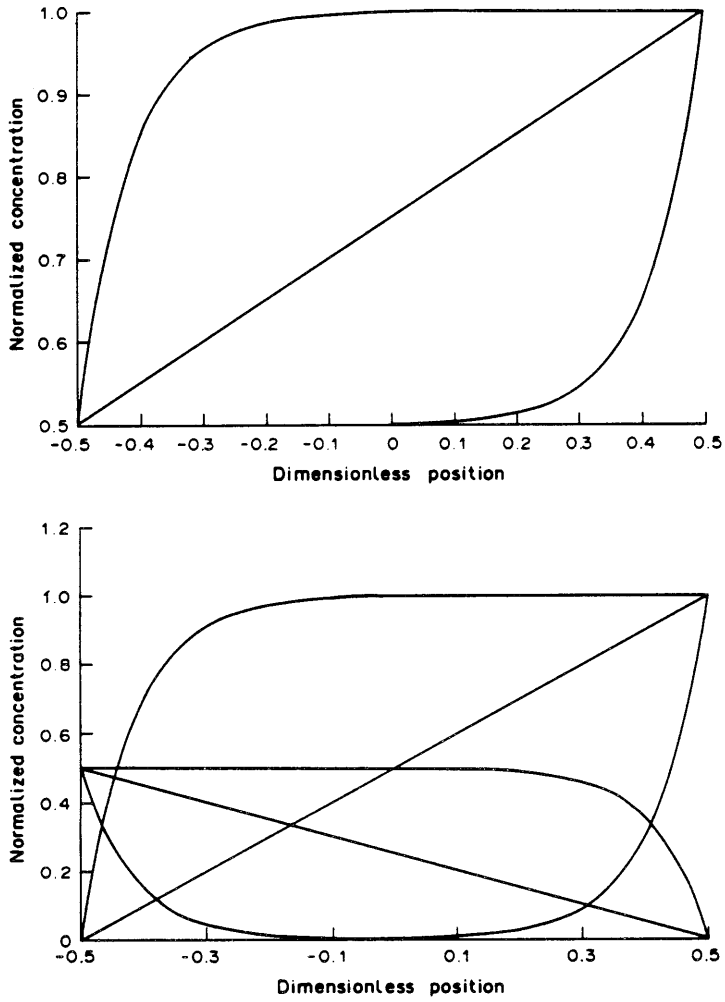

FIG. 14. Ion concentration as a function of position in a channel with a constant field potential. The normalized concentration in a constant field channel for $r_n = 2$ with transmembrane potential differences of -150, 0, 150. In the bottom panel the concentrations are broken down according to which side the ion entered.

(b) *Potentials with odd symmetry*

For the ramp potential, eqn (82) yields the following equation for the half saturation concentration in the small signal range:

$$n_{1/2} = \frac{1}{A\delta}\left(\frac{p}{\sinh(p)}\right). \tag{86}$$

Here, we have considered only the symmetric case where the concentration on the left end of the channel is equal to the concentration on the right end of the channel which is equal to the geometric average. Notice that $n_{1/2}$ is a decreasing function of the slope of the ramp, i.e. the larger the ramp the better the channel binds the ion. This is because (for $p > 0$) the increase in the channel's ability to bind ions entering the left more than compensates for the decrease in the channel's ability to bind ions entering from the right. This characteristic of the ramp potential emphasizes the vectorial nature of the channel affinity. From our experience with the independence and saturation fluxes, we might expect the ramp affinities to be related to the constant field affinities. This is the case and we again have that the sum of the affinities weighted by the Boltzmann factors at the ends of the channel is equal to the effective channel volume:

$$K_{al}e^{-p} + K_{ar}e^{p} = A\delta. \tag{87}$$

At zero transmembrane voltage, the affinity corresponding to ions entering the right end of the channel is smaller than the affinity corresponding to ions entering the left. Similarly the asymptotic results demonstrate the difference in the interaction between the channel and ions entering from one side versus the other:

$$n_{1/2} = \frac{e^p}{A\delta}\left[1 - \frac{1}{2u}(e^{-2p} - 1 - 4p)\right] + O(1/u^2), \quad u \gg 0 \tag{88}$$

$$n_{1/2} = \frac{e^{-p}}{A\delta}\left[1 + \frac{1}{2u}(e^{2p} - 1 + 4p)\right] + O1/u^2), \quad u \ll 0. \tag{89}$$

For positive voltages (ions drawn into the right end of the channel), the limiting half saturation concentration is larger than the constant field case by e^p but approaches from below due to the presence of the "well" at the left end of the channel. For negative voltages (ions drawn into the left end of the channel), the limiting half saturation concentration is smaller than the constant field case by e^{-p} but now approaches from above due to the "barrier" at the left end of the channel. This results in more rapid saturation of the current at negative voltages compared to positive voltages (Fig. 15) and an associated decrease in the rectification.

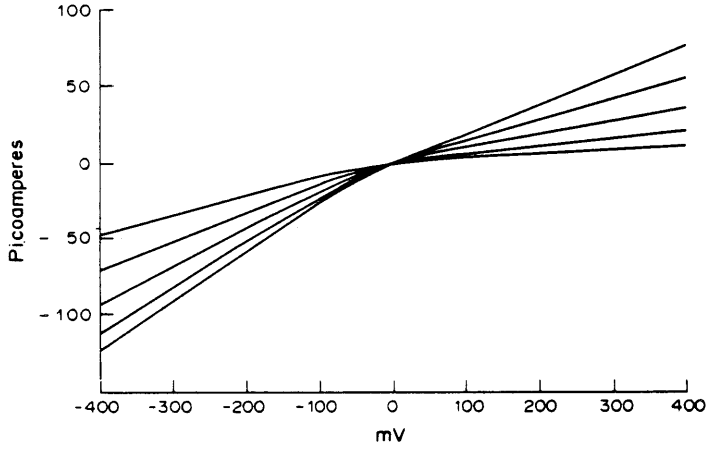

FIG. 15. Current–voltage–concentration surface for the ramp potential without access effects. The ramp potential with symmetric concentrations where the concentrations were varied in multiples of the equilibrium half saturation concentration $n = 4n_{0.5}$, $2n_{0.5}$, $n_{0.5}$, $n_{0.5}/2$, $n_{0.5}/4$ with the half saturation $n_{0.5} = 2.21$ M [eqn (87)]. Notice that the current saturates more rapidly at negative voltages which draw ions into the low potential end of the channel. This results in a current–voltage relationship which is more linear at high concentrations.

For the step potential with symmetric concentrations, the half saturation concentration in the small signal range is given by:

$$n_{1/2} = \frac{1}{A\delta \cosh(p)}. \tag{90}$$

Equation (90) shows that the half saturation concentration decreases more rapidly with the parameter p in the case of the step potential than in the case of the ramp potential. This is a result of the wider well on the left end of the channel compared to the ramp potential. For extreme voltages we have:

$$n_{1/2} \simeq \frac{e^p}{A\delta}\left(1 - \frac{1}{u} 2 \sinh^2(p)\right) + O(1/u^2), \quad u \gg 0 \tag{91}$$

$$n_{1/2} \simeq \frac{e^{-p}}{A\delta}\left(1 + \frac{1}{u} 2 \sinh^2(p)\right) + O(1/u^2), \quad u \ll 0. \tag{92}$$

The asymptotic results are qualitatively similar to the ramp potential but again the coefficients of $1/u$ contribute more due to the effectively wider well and barrier on the left and right ends of the channel respectively. This greater asymmetry in the voltage dependence of the half saturation for the step potential relative to the ramp potential explains the complete loss of rectification of the step potential saturation flux in symmetric concentrations mentioned in Section IV.

For the Z potential in the small signal range, we have the same result as for the ramp potential. For the asymptotic behavior, we have from eqns (80) and (81):

$$n_{1/2} = \frac{1}{A\delta}\left[1 - \frac{1}{2u}(e^{2p} - 1 - 2p)\right], \quad u \gg 0 \tag{93}$$

$$n_{1/2} = \frac{1}{A\delta}\left[1 + \frac{1}{2u}(e^{-2p} - 1 + 2p)\right], \quad u \ll 0. \tag{94}$$

Comparing eqns (88) and (89) with eqns (93) and (94), we see that the rate of approach to the asymptotic limits of the ramp and Z potentials are similar but due to the lack of an offset, the Z potential half saturation converges to the constant field limit. This result is similar but with opposite polarity to the corresponding independence fluxes. This results in the modest rectification of the Z independence flux near equilibrium being reversed by the larger asymmetry in Z potential saturation characteristics.

(c) *Single extremum potential*

In the small signal range we have:

$$n_{1/2} = \frac{1}{A\delta}\frac{pe^{p/2}}{2\sinh(p/2)}. \tag{95}$$

As one would expect, for a well (p negative), the half saturation concentration decreases exponentially with the depth of the well. However, for a barrier (p positive), the half saturation concentration grows only linearly with the height of the barrier. Far away from equilibrium, the half saturation concentration can be approximated by eqns (80) and (81) and we have:

$$n_{1/2} \simeq \frac{1}{A\delta}(1 + p/|u|). \tag{96}$$

From eqn (96), we see that at extreme voltages the half saturation concentration approaches the constant field result with a hyperbolic dependence on the voltage. When p is negative, the half saturation concentration approaches the constant field value from below and when p is positive, the half saturation concentration approaches the constant field value from above. These results are illustrated in Fig. 16. In the case of a well, this results in a more rapid saturation near equilibrium than at extreme voltages which results in a transition from a sublinear to a superlinear current–voltage relationship with increasing concentration. In Fig. 17, panel 1 we have plotted the current–voltage–concentration surface for a $3k_bT$ well. The modest depth of the well results in an extremely linear current–voltage relationship even out to 400 mV of applied voltage. In the case of a barrier, saturation is more rapid at extreme voltages relative to the small signal range. This results in the superlinear current–voltage relationship throughout the concentration range seen in Fig. 17, panel 2.

2. *Channel Affinity in the Presence of Access Effects*

There are two effects due to access limitations on the channel affinity. The first effect is completely analogous to the discussion of the independence flux in Section III. This effect can be accounted for by multiplying the affinities by the resistance ratio. This results in a

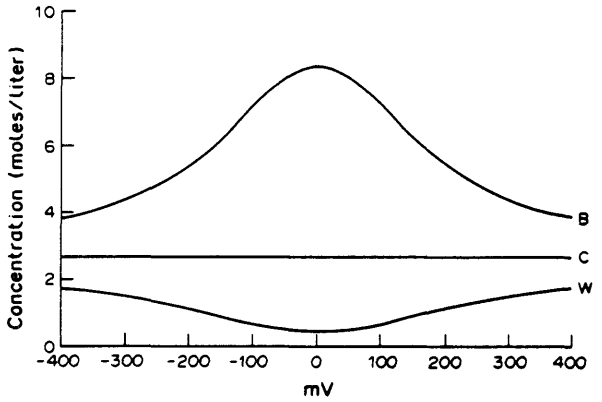

FIG. 16. Comparison of the voltage dependence of the constant field, $3k_bT$ barrier and $3k_bT$ well half saturation concentrations without access effects. The effects of the high channel affinity of the well and low channel affinity of the barrier potentials are manifested in the low half saturation concentration of the well and high half saturation concentration of the barrier. At extreme voltages in the absence of access effects the well and barrier converge to the constant field case.

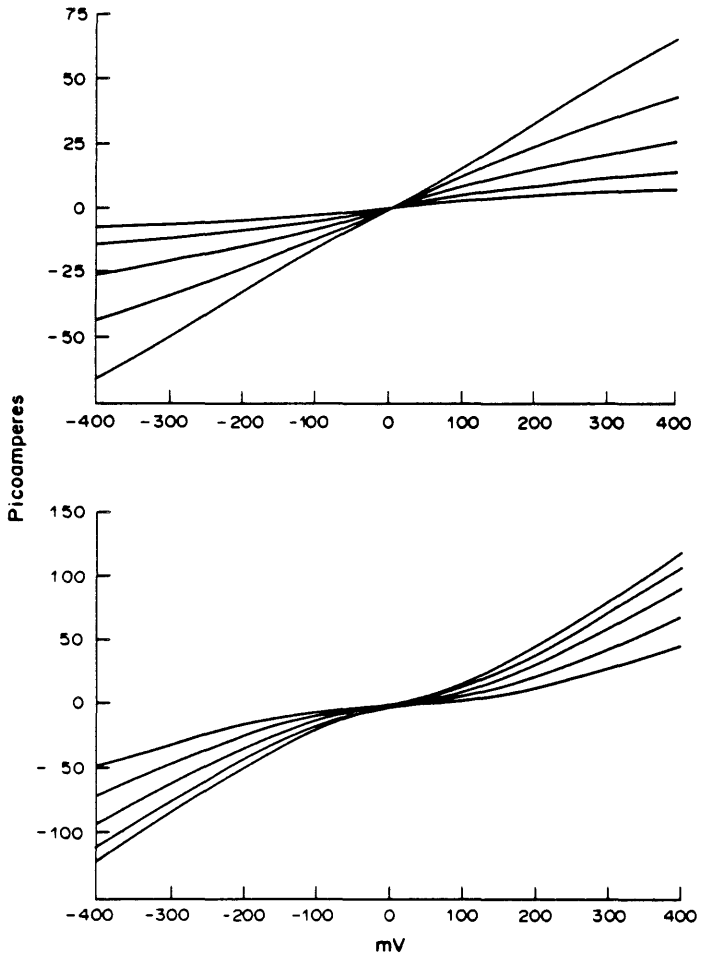

FIG. 17. Current–voltage–concentration surface for the well and barrier potentials without access effects. Panel 1: the current–voltage–concentration surface for the $3k_bT$ well potential with symmetric concentrations with and $n = n_{0.5}/4$, $n_{0.5}/2$, $n_{0.5}$, $2n_{0.5}$, $4n_{0.5}$, with the half saturation concentration $n_{0.5} = 0.415$ M [calculated using eqn (96)]; panel 2: plot of the $3k_bT$ barrier current–voltage–concentration surface analogous to panel 1. In this case the equilibrium half saturation concentration is $n_{0.5} = 8.28$ M. In the case of the well there is a change in the concavity with increasing concentration from sub- to superlinearity in contrast to the barrier potential which is superlinear at all concentrations.

decrease in the channel affinity to ions at large voltages. The other effect is an increased occupancy time due to reentries.

VI. DISCUSSION

The major result of this paper is eqn (23). This equation is a generalization of a result previously derived by Levitt (1986). It generalizes to the case where access resistances are not negligible. In addition to this generalization, we have introduced several conceptual tools to help understand this model. These include mean first passage times, mean occupancy times, independence flux, saturation flux and affinity constants. We have used these concepts to understand the behavior of eqn (23) for a set of simple potential profiles. By analyzing the limiting behavior near equilibrium and at large voltages we can intuit the major features of the current–voltage relationship. From the asymptotic analysis at large voltages, it becomes clear that the offset and slope of the potential profile at the channel mouths are of primary importance. This motivated our choice of potential profiles. The major results of this analysis are summarized in Tables 1 and 2.

We have chosen three major aspects of this model to present in detail. These aspects are: the effects of access resistance, the causes of rectification, and the basis of the linearity of the current–voltage relationship. The primary effect of access limitations is to cause the current to saturate with increasing voltage. This is due to the eventual limitation of the rate at which ions can be supplied to the channel from the baths. Recent experiments imply that such access limitations may be important in channel behavior (Laver *et al.*, 1989). Note that our analysis has assumed voltage independent entrance rates; recently this assumption has been called into question for the gramicidin channel (Hainsworth and Hladky, 1987).

In Section III we discussed three sources of rectification in the independence flux. The first type discussed was the well known Goldman constant field rectification. This is the rectification one sees in a structureless channel when asymmetric concentrations are placed across it. This type of rectification should exist in any channel well below its saturation level. The remaining two types of rectification are consequences of asymmetries in the potential profile of the channel. Any asymmetric profile should produce some rectification but here we are concerned only with the rectification related to the first three terms of an asymptotic expansion associated with extreme voltages. In this case the asymptotic analysis shows that the offset and slope of the potential profile at the channel mouths are the major factors determining rectification. Various combinations of these factors were investigated with the different choices of potentials we considered.

The final theme we developed is the linearity of the model. We observe that the full one-ion model is more linear than the independence case, i.e. ion–ion interaction linearizes the current–voltage relationship. The basis of this linearity can be approached in three complimentary ways. Mathematically, the linearity is a result of the dependence of J_s on passage times, while J_i depends only on electrodiffusive resistances. A second way of thinking about this linearization is that ions can enter the low potential side of the channel easily but have trouble traversing the channel because they are moving against the potential. This asymmetry tends to even out the intrinsic rectification that the potential profile gives in the independence case. Finally, but in a related way, rectification is decreased by the fact that the current saturates with concentration more quickly for ions that enter from the low potential side.

An issue of more practical importance for modelling channels is the observation that diffusion models seem to give more linear current–voltage relationships than do Eyring models, given the same potential profiles. Clearly, one can fit a linear current–voltage relationship with an Eyring model but it will require more barriers and wells than a diffusion model would (Levitt, 1986). This raises the issue of the uniqueness of interpretation of features of the potential profile. If different models fit the same data with different potential functions, which if any corresponds to the "real" profile, or is it a matter of how you interpret the features in the different models?

As mentioned in the introduction, this theory is presented primarily as a conceptual tool to be used in developing intuition about the behavior of diffusion models. There are enough

limitations to this theory that it is unlikely to be an accurate model of any real channel. The most important limitation is that of one-ion occupancy. As channels are investigated in more detail, it is becoming clear that there may not be any channel that is so constructed that it absolutely limits occupancy to a single ion. It could be said that this theory describes the behavior of real channels in the low concentration limit. While this is certainly true, there is an important practical issue involved. The concentration range over which a real channel is effectively one-ion may be so small that measuring current may not be practical because of signal to noise limitations.

At high concentrations (approaching J_s), any real channel would probably begin to have a significant fraction of multiple occupancies. To correctly predict at what concentration this occurs would require a full two-ion diffusion theory (Levitt, 1987). However, we can do an approximate calculation by treating the equilibrium case. Assume that the channel can only be in one of three possible states: empty, occupied by one ion, or occupied by two ions. Under this assumption we have for the channel occupancy probabilities (Gates *et al.*, 1990):

$$P_0 = \frac{1}{\sum} \tag{97}$$

$$P_1 = \frac{nA}{\sum} \int_{-\delta/2}^{\delta/2} e^{-\phi_1(x)}\, dx \tag{98}$$

$$P_2 = \frac{(nA)^2}{\sum} \int_{2r}^{\delta/2} \int_{-\delta/2}^{x_1 - 2r} e^{-\phi_2(x_1, x_2)}\, dx_2\, dx_1 \tag{99}$$

$$\sum = 1 + nA \int_{-\delta/2}^{\delta/2} e^{-\phi_1(x)}\, dx + (nA)^2 \int_{2r}^{\delta/2} \int_{-\delta/2}^{x_1 - 2r} e^{-\phi_2(x_1, x_2)}\, dx_2\, dx_1 \tag{100}$$

where ϕ is the dimensionless potential, x_1 is the distance from the left end of the channel of the right-most ion, x_2 is the distance from the left end of the channel of the other ion (only one half of the available configurations are included since there are two ways to label the two particles), $2r$ is the closest distance of approach between the two ions, A is the cross sectional area of the channel which is accessible to the permeant ion, and n is the concentration of permeant ion in the bath at the reference potential ($\phi = 0$).

We must now specify the potential functions in eqns (98) through (100). We assume that the interaction potential between the channel and each ion superposes with the potential of interaction between two ions (that is, the binding of the two ions is not cooperative in any way). Thus, the one-ion potential, ϕ_1, is the ion–channel interaction potential. The two ion potential, ϕ_2, is the sum of the ion–channel interaction potential at x_1 plus the ion channel interaction potential at x_2 plus the ion–ion interaction potential $\phi_i(x_1, x_2)$. We use the simplified version of Levitt's (1985) ion–ion interaction potential described in Gates *et al.* (1990). Thus, we have:

$$\phi_2(x_1, x_2) = \phi_1(x_2) + \phi(x_1, x_2) \tag{101}$$

$$\phi_i(x_1, x_2) = \frac{z_1 z_2 e^2}{\pi \rho^2 \kappa \varepsilon_0 k_b T} \left[\frac{(\eta + x_2)(\eta + \delta - x_1)}{2\eta + \delta} \right] \tag{102}$$

where, η is a length defined by:

$$\eta = \frac{1}{1/\lambda + 1/\rho}, \tag{103}$$

ρ is the channel radius and λ is the Debye length.

We compare the results of the above analysis for a centrally located well vs a centrally located barrier. If we take the dielectric constant to be 50 with a one-ion affinity constant of $(100\ \text{mM})^{-1}$, we obtain the results in Fig. 18. Clearly, there exists a range of concentrations over which the one-ion assumption is a reasonable approximation for the well. For the

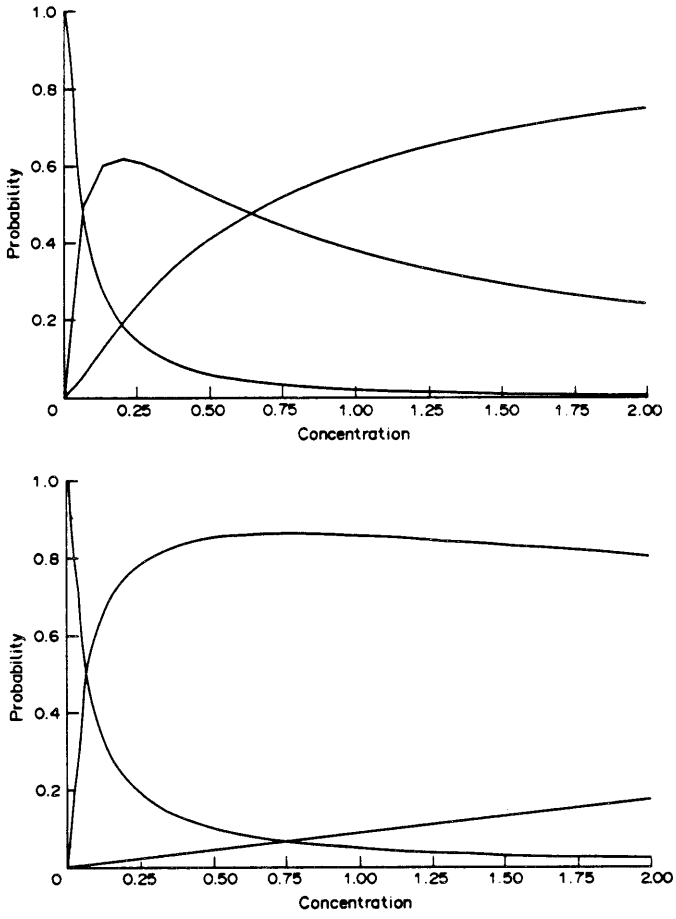

FIG. 18. Occupancy vs concentration. Panel 1: the equilibrium probabilities that a channel with a $3k_bT$ well will be occupied by zero, one, or two ions. The dielectric constant of eqn (102) is set to 50 and the potential is offset so that the one ion affinity of eqn (96) is equal to 0.1 M; panel 2: the analogous plot for the $3k_bT$ barrier. The large negative offset necessary to match the one ion affinity of the barrier with the well effectively produces a binding site at each end of the channel separated by a $3k_bT$ barrier. This means that the ion–channel interactions stabilize configurations which minimize ion–ion interactions and the channel is occupied by two ions almost 20% of the time at 200mM. In the case of the well the ion–channel interactions stabilize configurations which enhance ion–ion interactions and so an order of magnitude higher concentration is required to achieve double occupancy compared to the barrier.

barrier, there is no such range. The reader should be cautioned that this is only an order of magnitude estimate of the effects of double occupancy. For example, multiple occupancy in the well potential would be expected to have a greater influence on the flux than in the barrier potential.

Another major aspect of channel protein behavior left out of this model has to do with our assumption of a unique function $\phi^0(x)$ describing the ion–channel interaction potential. A channel protein may well undergo conformational changes on a time scale that would have significant effects on ion permeation. Such behavior can cause a single-ion channel to behave like a multi-ion channel (Lauger, 1985). Conceptually such phenomena can easily be incorporated into this theory, but this leads to considerable computational complexity.

There are two other subtle assumptions in this theory that may not be obvious to the reader. We have discussed them at length elsewhere (Gates *et al.*, 1990). Our entire approach has been based on the assumption of steady-state behavior, i.e. we assume that when an ion enters or exits a channel the bath filling rate relaxes instantaneously to its steady-state value. This may not be so. If not, the proper boundary conditions would be found from the solution of a time dependent diffusion problem. There is also a hidden assumption of independent particle behavior involved in reentrances. When we calculate the probability of an exiting particle reentering, we do not take into account the possibility that a different particle might

enter the channel during the period between reentrances. The issue of quantum identifiability enters here.

Future development of this theory requires treatment of all the above issues. This becomes increasingly difficult and the resulting analytical theories become increasingly cumbersome. At some point, machine calculation may be more efficient or at least a useful adjunct to the analytical work. A great deal of progress is being made on that front (Furois-Corbin and Pullman, 1989; Chiu *et al.*, 1989; Jordan, 1989).

VII. APPENDICES

1. *Asymptotic Properties of Electrodiffusive Resistances and MFPTs*

In this appendix we consider the asymptotic behavior of the one-ion diffusion theory. We will demonstrate the method with two examples; the asymptotic behavior of the electrodiffusive resistance, R_c, and the mean first passage times τ_l and τ_r. These results can then be used to characterize the asymptotic behavior of the three components (J_i, J_s and $\bar{n}_{1/2}$) of the one-ion diffusion theory.

The problem at hand is one of determining the asymptotic behavior of a definite integral which depends on a parameter different from the variables of integration. In this particular case the parameter in question is the voltage difference across the membrane in which the channel is located. Hence, the results of this appendix will yield the limiting behavior of these integrals at extreme transmembrane voltages.

The first case we consider will be the integral in the expression for the channel electrodiffusive resistance [i.e. the denominator of eqn (11)]:

$$\int_{-\delta/2}^{\delta/2} e^{\phi(x)}\,dx. \tag{A1}$$

We make the same assumption of superposition as made in eqn (41). Under this assumption integral (A1) can be written:

$$\int_{-\delta/2}^{\delta/2} f(x)e^{\Delta\phi x/\delta}\,dx. \tag{A2}$$

Here, we define $f(x)=e^{\phi^0(x)}$. Repeated integration of (A2) by parts yields:

$$\begin{aligned}&\frac{\delta}{\Delta\phi}\left(e^{\Delta\phi/2}f(\delta/2)-e^{-\Delta\phi/2}f(-\delta/2)\right)\\&-\left(\frac{\delta}{\Delta\phi}\right)^2\left(e^{\Delta\phi/2}f_x(\delta/2)-e^{-\Delta\phi/2}f_x(-\delta/2)+\Delta f(0)\right)\\&+\left(\frac{\delta}{\Delta\phi}\right)^3\left(e^{\Delta\phi/2}f_{xx}(\delta/2)-e^{-\Delta\phi/2}f_{xx}(-\delta/2)+\Delta f_x(0)\right)+O(1/\Delta\phi)^4\end{aligned} \tag{A3}$$

where f_x and f_{xx} denote the first and second derivatives of f with respect to x, and $\Delta f(0)$ and $\Delta f_x(0)$ are jumps which occur in f and its first derivative at $x=0$. To illustrate the method by which jumps are handled we consider an approximating potential where the sudden transition at $x=0$ occurs over a ramp of length 2ε. For example, the step potential can be approximated by $\phi^0(x)=-p$ for $-\delta/2\le x\le-\varepsilon$, $\phi^0(x)=px/\varepsilon$ for $-\varepsilon<x<\varepsilon$, and $\phi^0(x)=p$ for $\varepsilon\le x\le\delta/2$. The above repeated integration by parts is then carried out for each of the three regions. Finally, when the limit is taken as ε goes to zero the ramp in the potential becomes an impulse in the derivative of the potential at zero. This impulse is a scalar multiple of the well known Dirac delta function. The delta function can be defined as the derivative of the unit step function. Consequently the magnitude of this impulse is the magnitude of the jump in ϕ.

We now consider the two limits as $\Delta\phi\to\pm\infty$. When $\Delta\phi$ becomes large and positive we have, out to third order in $1/\Delta\phi$, the following approximation:

$$\left[\frac{\delta}{\Delta\phi}-\left(\frac{\delta}{\Delta\phi}\right)^2\phi_x^0(\delta/2)+\left(\frac{\delta}{\Delta\phi}\right)^3\{(\phi_x^0(\delta/2))^2+\phi_{xx}^0(\delta/2)\}\right]\mathrm{f}(\delta/2)\mathrm{e}^{\Delta\phi/2}. \tag{A4}$$

When $\Delta\phi$ becomes large in absolute value and negative we have:

$$-\left[\frac{\delta}{\Delta\phi}-\left(\frac{\delta}{\Delta\phi}\right)^2\phi_x^0(-\delta/2)+\left(\frac{\delta}{\Delta\phi}\right)^3\{(\phi_x^0(-\delta/2))^2+\phi_{xx}^0(-\delta/2)\}\right]\mathrm{f}(-\delta/2)\mathrm{e}^{-\Delta\phi/2}. \tag{A5}$$

Combining eqns (38) and (A4) we have for the asymptotic properties of the independence flux at positive transmembrane voltages:

$$-J=\frac{AD}{\delta}n(\delta/2)\mathrm{e}^{-\phi^0(\delta/2)}\left(\Delta\phi+\delta\phi_x^0(\delta/2)-\frac{\delta^2}{\Delta\phi}\phi_{xx}^0(\delta/2)\right)+O(1/\Delta\phi^2). \tag{A6}$$

Similarly, combining eqns (38) and (A5) we have at negative transmembrane voltages:

$$-J=\frac{AD}{\delta}n(-\delta/2)\mathrm{e}^{-\phi^0(-\delta/2)}\left(\Delta\phi+\delta\phi_x^0(-\delta/2)-\frac{\delta^2}{\Delta\phi}\phi_{xx}^0(-\delta/2)\right)+O(1/\Delta\phi^2). \tag{A7}$$

Notice that the asymptotic results depend on the characteristics of the potential at the ends of the channel and so a jump in the center of the channel only influences the properties of the independence flux near equilibrium. If we assume that the curvature of the potential profiles at the ends of the channel is small we have, out to terms that decay with $1/(\Delta\phi^2)$, that the independence flux at extreme voltages is linear with the slope and intercept given by:

$$\text{slope}=\frac{AD}{\delta}n(a)\mathrm{e}^{-\phi^0(a)} \tag{A8}$$

$$\text{intercept}=ADn(a)\frac{\mathrm{d}}{\mathrm{d}x}\phi^0(a)\mathrm{e}^{-\phi^0(a)} \tag{A9}$$

where $a=-\delta/2$ and $\delta/2$ at negative and positive transmembrane voltages respectively.

We now consider the integral expressions of the mean first passage time τ_l. Our treatment will initially consider the case where $\phi^0(x)$ and all of its derivatives are continuous. After completing this analysis we will outline a method by which jump discontinuities can be handled. Combining the definition of the electrodiffusion resistance in eqn (11) with eqn (20) we have:

$$\tau_l=\frac{1}{D}\int_{-\delta/2}^{\delta/2}\int_y^{\delta/2}\mathrm{e}^{\phi^0(x)-\phi^0(y)}\mathrm{e}^{\Delta\phi(x-y)/\delta}\,\mathrm{d}x\,\mathrm{d}y. \tag{A10}$$

This is a double integral over a triangular region in the x–y plane. We make use of the following change of coordinates:

$$\eta=\frac{1}{\delta}(y-x)\qquad y=\frac{\delta}{2}(\eta+\xi)$$

$$\xi=\frac{1}{\delta}(y+x)\qquad x=\frac{\delta}{2}(\xi-\eta).$$

The region in the η–ξ plane is illustrated in Fig. 19. Equation (A10) can now be written as a double integral in the η–ξ plane to yield:

$$\tau_l=\frac{\delta^2}{2D}\left(\int_{-1}^{0}\int_{-\xi}^{0}\mathrm{f}(\eta,\xi)\mathrm{e}^{-\Delta\phi\eta}\mathrm{d}\eta\mathrm{d}\xi+\int_0^1\int_{\xi-1}^{0}\mathrm{f}(\eta,\xi)\mathrm{e}^{-\Delta\phi\eta}\,\mathrm{d}\eta\,\mathrm{d}\xi\right)$$

$$\mathrm{f}(\eta,\xi)=\exp[\phi^0\{x(\eta,\xi)\}-\phi^0\{y(\eta,\xi)\}]. \tag{A11}$$

If we now consider the integrals of eqn (A11) to be iterated we notice that the first integration

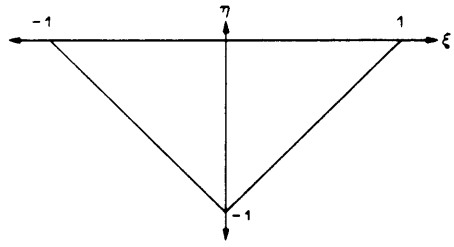

FIG. 19. Region of integration in the η, ξ plane for the MFPT τ_l.

is of the form of integral (A2). The linearity of integration allows for an exchange in the order of sum and integration and we have for the first integral on the right hand side of eqn (A9):

$$-\frac{\delta^2}{2D\Delta\phi}\int_{-1}^{0} d\xi(f(0,\xi)-e^{\Delta\phi(\xi+1)}f(-\xi-1,\xi))$$
$$-\frac{\delta^2}{2D}\left(\frac{1}{\Delta\phi}\right)^2\int_{-1}^{0} d\xi(f_\eta(0,\xi)-e^{\Delta\phi(\xi+1)}f_\eta(-\xi-1,\xi))$$
$$-\frac{\delta^2}{2D}\left(\frac{1}{\Delta\phi}\right)^3\int_{-1}^{0} d\xi(f_{\eta\eta}(0,\xi)-e^{\Delta\phi(\xi+1)}f_{\eta\eta}(-\xi-1,\xi))+O(1/\Delta\phi^4). \quad \text{(A12)}$$

Likewise we have for the second integral on the right hand side of eqn (A11):

$$-\frac{\delta^2}{2D\Delta\phi}\int_{-1}^{0} d\xi(f(0,\xi)-e^{-\Delta\phi(\xi-1)}f(\xi-1,\xi))$$
$$-\frac{\delta^2}{2D}\left(\frac{1}{\Delta\phi}\right)^2\int_{-1}^{0} d\xi(f\eta(0,\xi)-e^{-\Delta\phi(\xi-1)}f_\eta(\xi-1,\xi))$$
$$-\frac{\delta^2}{2D}\left(\frac{1}{\Delta\phi}\right)^3\int_{-1}^{0} d\xi(f_{\eta\eta}(0,\xi)-e^{-\Delta\phi(\xi-1)}f_{\eta\eta}(\xi-1,\xi))+O(1/\Delta\varphi^4). \quad \text{(A13)}$$

We again perform a repeated integration by parts of the second terms in the brackets of eqns (A12) and (A13) and combine the results to yield:

$$\tau_l=\frac{\delta^2}{2D}\left\{-\frac{1}{\Delta\varphi}\int_{-1}^{1} d\xi f(0,\xi)+\left(\frac{1}{\Delta\phi}\right)^2\left[2e^{\Delta\phi}f(-1,0)-f(0,-1)-f(0,1)-\int_{-1}^{1} d\xi f_\eta(0,\xi)\right]\right.$$
$$+\left(\frac{1}{\Delta\phi}\right)^3\left[e^{\Delta\phi}[f_\eta(-1,0,-\pi/4)+f_\eta(-1,0,-3\pi/4)+f_\xi(-1,0,-\pi/4)-f_\xi(-1,0,-3\pi/4)]\right.$$
$$\left.\left.-f_\eta(0,-1)-f_\eta(0,1)+f_\xi(0,-1)-f_\xi(0,1)-\int_{-1}^{1} d\xi f_{\eta\eta}(0,\xi)\right]\right\}+O(1/\Delta\phi^4). \quad \text{(A14)}$$

We have included the angle in radians of the vector describing the direction of the contour along which the second integration takes place. This is necessary to distinguish between the two cases for each partial derivative with respect to η and ξ. We return to this issue below when computing the derivatives. Preserving only coefficients of $e^{\Delta\phi}$, we have the asymptotic behavior for positive values of the transmembrane voltage:

$$\tau_l=\frac{1}{2D}\left(\frac{\delta}{\Delta\phi}\right)^2\left[2f(-1,0)\right.$$
$$\left.+\frac{1}{\Delta\phi}[f_\eta(-1,0,-\pi/2)+f_\eta(-1,0,-3\pi/2)+f_\xi(-1,0,-\pi/2)-f_\xi(-1,0,-3\pi/2)]\right]e^{\Delta\phi}. \quad \text{(A15)}$$

For $f(-1,0)$ we have:

$$f(-1, 0) = e^{\Delta\phi^0} \tag{A16}$$

with

$$\Delta\phi^0 = \phi^0(\delta/2) - \phi^0(-\delta/2).$$

For $f_\eta(-1, 0, -3\pi/4)$, we take η to be the independent variable and we have the case where $\xi(\eta) = \eta + 1$. For $f_\eta(-1, 0, -\pi/4)$ we have the case where $\xi(\eta) = -\eta - 1$. Similarly for $f_\xi(-1, 0, -3\pi/4)$ and $f_\xi(-1, 0, -\pi/4)$, we take ξ to be the independent variable and we have: $\eta(\xi) = \xi - 1$ and $\eta(\xi) = -\xi - 1$ respectively. As an example we consider the two cases for the partial derivative of f with respect to η. When $\eta = -1$ and $\xi = 0$, $x = \delta/2$ and $y = -\delta/2$ and we have:

$$\begin{aligned} f_\eta(-1, 0, -3\pi/4) &= \frac{\partial}{\partial\eta} f[x\{\eta(\eta), \xi(\eta)\}, y\{\eta(\eta), \xi(\eta)\}]|_{\eta=-1,\ \xi=\eta+1} \\ &= \left[\frac{\partial f}{\partial x}\frac{\partial x}{\partial \eta}\frac{\partial \eta}{\partial \eta} + \frac{\partial f}{\partial x}\frac{\partial x}{\partial \xi}\frac{\partial \xi}{\partial \eta} + \frac{\partial f}{\partial y}\frac{\partial y}{\partial \eta}\frac{\partial \eta}{\partial \eta} + \frac{\partial f}{\partial y}\frac{\partial y}{\partial \xi}\frac{\partial \xi}{\partial \eta}\right]_{\eta=-1,\ \xi=\eta+1} \\ &= -\delta\phi^{0'}(y) f(x, y)|_{x=\delta/2,\ y=-\delta/2} = -\delta\phi^{0'}(-\delta/2)e^{\Delta\phi^0} \end{aligned} \tag{A17}$$

$$\begin{aligned} f_\eta(-1, 0, -\pi/4) &= \frac{\partial}{\partial\eta} f[x\{\eta(\eta), \xi(\eta)\}, y\{\eta(\eta), \xi(\eta)\}]|_{\eta=-1,\ \xi=-\eta-1} \\ &= \left[\frac{\partial f}{\partial x}\frac{\partial x}{\partial \eta}\frac{\partial \eta}{\partial \eta} + \frac{\partial f}{\partial x}\frac{\partial x}{\partial \xi}\frac{\partial \xi}{\partial \eta} + \frac{\partial f}{\partial y}\frac{\partial y}{\partial \eta}\frac{\partial \eta}{\partial \eta} + \frac{\partial f}{\partial y}\frac{\partial y}{\partial \xi}\frac{\partial \xi}{\partial \eta}\right]_{\eta=-1,\ \xi=-\eta-1} \\ &= -\delta\phi^{0'}(x) f(x, y)|_{x=\delta/2,\ y=-\delta/2} = -\delta\phi^{0'}(\delta/2)e^{\Delta\phi^0}. \end{aligned} \tag{A18}$$

Similarly,

$$f_\xi(-1, 0, -3\pi/4) = -\delta\phi^{0'}(-\delta/2)e^{\Delta\phi^0} \tag{A19}$$

$$f_\xi(-1, 0, -\pi/2) = \delta\phi^{0'}(\delta)e^{\Delta\phi^0}. \tag{A20}$$

Combining eqns (A17) through (A20) with eqn (A15) yields:

$$\tau_l \simeq \frac{1}{D}\left(\frac{\delta}{\Delta\phi}\right)^2\left[1 - \frac{\delta}{\Delta\phi}(\phi^{0'}(\delta/2) + \phi^{0'}(-\delta/2))\right]e^{\Delta\phi + \Delta\phi^0}. \tag{A21}$$

This result predicts an exponential dependence of the rate of escape from the reflecting boundary to the absorbing boundary. This is qualitatively similar to Kramers' (1940) result and thus to traditional rate theory (also see Cooper *et al.*, 1988b).

We also mention that eqn (A21) remains correct in the case where there is a jump in the potential in the center of the channel. This is due to the fact that the asymptotic properties of the passage time are dominated by the features of the surface in the neighborhood of the point $\eta = -1$, $\xi = 0$. As we shall see later, a jump in the potential at the center of the channel does not directly influence this part of the surface.

At negative transmembrane voltages eqn (A11) becomes:

$$\begin{aligned} \tau_l \simeq \frac{\delta^2}{2D}\Bigg\{ &-\frac{1}{\Delta\phi}\int_{-1}^{1} d\xi f(0, \xi) - \left(\frac{1}{\Delta\phi}\right)^2\left[f(0, -1) + f(0, \xi) + \int_{-1}^{1} d\xi f_\eta(0, \xi)\right] \\ &-\left(\frac{1}{\Delta\phi}\right)^3\left[f_\eta(0, -1) + f_\eta(0, 1) - f_\xi(0, -1) + f_\xi(0, 1) + \int_{-1}^{1} d\xi f_{\eta\eta}(0, \xi)\right]\Bigg\} + O(1/\Delta\phi^{n+1}). \end{aligned} \tag{A22}$$

For the first partial derivatives of f we have:

$$f_\eta(0, \xi) = -\delta\frac{d}{dx}\phi^0(x) \tag{A23}$$

$$f_\eta(0, -1) = -\delta\phi^{0'}(-\delta/2) \tag{A24}$$

$$f_\eta(0, 1) = -\delta\phi^{0'}(\delta/2) \tag{A25}$$

$$f_\xi(0, -1) = \delta\phi^{0'}(-\delta/2) \tag{A26}$$

$$f(0, 1) = -\delta\phi^{0'}(\delta/2). \tag{A27}$$

The second partial derivative with respect to η is:

$$f_{\eta\eta}(0, \xi) = \left(\delta \frac{d}{dx}\phi^0(x)\right)^2. \tag{A28}$$

Substituting x for ξ in the fourth term of the right hand side of approximation (A22) with $\eta = 0$ and making use of eqn (A23) yields:

$$\int_{-1}^{1} d\xi f_\eta(0, \xi) = -2\int_{-\delta/2}^{\delta/2} d\phi^0. \tag{A29}$$

A similar result holds for $f(0, \xi)$ and $f_{\eta\eta}(0, \xi)$. Combining eqns (A23) through (A29) with eqn (A22) we have for negative values of the transmembrane voltage:

$$\tau_l \simeq \frac{1}{D}\left(\frac{\delta}{\Delta\phi}\right)^2\left[-\Delta\phi + \Delta\phi^0 - 1 + \frac{\delta}{\Delta\phi}\left(\phi^{0'}(-\delta/2) + \phi^{0'}(\delta/2) - \int_{-\delta/2}^{\delta/2}[\phi^{0'}(x)]^2 dx\right)\right]. \tag{A30}$$

Applying the same procedure for τ_r for the asymptotic behavior at negative transmembrane voltages, we obtain:

$$\tau_r \simeq \frac{1}{D}\left(\frac{\delta}{\Delta\phi}\right)^2\left[1 - \frac{\delta}{\Delta\phi}(\phi^{0'}(\delta/2) + \phi^{0'}(-\delta/2))\right] e^{-\Delta\phi - \Delta\phi^0}. \tag{A31}$$

For asymptotic behavior at positive transmembrane voltages we have:

$$\tau_r \simeq \frac{1}{D}\left(\frac{\delta}{\Delta\phi}\right)^2\left[\Delta\phi - \Delta\phi^0 - 1 + \frac{\delta}{\Delta\phi}\left(\phi^{0'}(-\delta/2) + \phi^{0'}(\delta/2) + \int_{-\delta/2}^{\delta/2}[\phi^{0'}(x)]^2\, dx\right)\right]. \tag{A32}$$

The above analysis was for continuous potentials. We now extend it to include potentials with jumps. In both cases the asymptotic properties of the MFPTs are dominated by the features of the η, ξ surface in the neighborhood of line $\eta = 0$. To include the effects of jumps, we proceed as we did in the one dimensional case except the ramp now defines four contours: $\eta = \xi + \varepsilon$, $\eta = \xi - \varepsilon$, $\eta = -\xi + \varepsilon$, and $\eta = -\xi - \varepsilon$. in the case of τ_l, these contours define six regions of the η, ξ surface. Applying these contours to Fig. 19 we can see that the influence on eqns (A30) and (A32) will be from the neighborhood of the point $\eta = 0$, $\xi = 0$. If we carry out the integration by parts over each region and then pass to the limit as ε goes to zero we obtain additional terms for eqn (A30):

$$\frac{1}{D}\left(\frac{\delta}{\Delta\phi}\right)^2 (e^{\Delta\phi_j} - 1 - \Delta\phi_j) \tag{A33}$$

and for eqn (A32):

$$\frac{1}{D}\left(\frac{\delta}{\Delta\phi}\right)^2 (e^{-\Delta\phi_j} - 1 + \Delta\phi_j). \tag{A34}$$

Here, we define $\Delta\phi_j$ as the magnitude of the jump.

Combining eqn (59) with eqns (A21) and (A32), we obtain the positive voltage asymptote of J_s:

$$-J_s = \frac{D}{\delta^2}\left[\Delta\phi - \beta_p + \frac{1}{\Delta\phi}(\beta_p^2 - \gamma)\right]$$

$$\beta_p = \frac{1}{r_n} e^{\Delta\phi^0} - 1 - \Delta\phi^0 + e^{-\Delta\phi_j} - 1 + \Delta\phi_j$$

$$\gamma_p = \delta\left[\left(\frac{r_n - e^{\Delta\phi^0}}{r_n}\right)(\phi^{0'}(\delta/2) + \phi^{0'}(-\delta/2)) + \int_{-\delta/2}^{\delta/2}[\phi^{0'}(x)]^2\, dx\right]. \tag{A35}$$

For negative voltages we combine eqn (59) with eqns (A30) and (A31) to yield:

$$-J_s = \frac{D}{\delta^2}\left[\Delta\phi - \beta_n + \frac{1}{\Delta\phi}(\beta_n^2 - \gamma_p)\right]$$

$$\beta_n = -r_n e^{-\Delta\phi^0} + 1 - \Delta\phi^0 - e^{\Delta\phi_j} + 1 + \Delta\phi_j$$

$$\gamma_n = -\delta\left[(1 - r_n e^{-\Delta\phi^0})(\phi^{0'}(\delta/2) + \phi^{0'}(-\delta/2)) - \int_{-\delta/2}^{\delta/2} [\phi^{0'}(x)]^2\, dx\right]. \tag{A36}$$

Combining eqns (A4), (A21), (A32) with eqn (75) for the half saturation concentration we have for large positive voltages:

$$\bar{n}_{1/2} \simeq \frac{1}{\delta A\sqrt{r_n}} e^{\phi^0(\delta/2)}\left[1 - \frac{1}{\Delta\phi}(\delta\phi^{0'}(\delta/2) + \beta_p)\right.$$

$$\left. + \frac{1}{\Delta\phi^2}(\delta^2[\phi^{0'}(\delta/2)^2 + \phi^{0''}(\delta/2)] - \gamma_p + \delta\phi^{0'}(\delta/2)\beta_p + \beta_p^2)\right]. \tag{A37}$$

For large negative voltages we use eqns (A4), (A30), (A31) with eqn (75) to yield:

$$\bar{n}_{1/2} \simeq \frac{\sqrt{r_n}}{\delta A} e^{\phi^0(-\delta/2)}\left[1 - \frac{1}{\Delta\phi}(\delta\phi^{0'}(-\delta/2) + \beta_n)\right.$$

$$\left. + \frac{1}{\Delta\phi^2}(\delta^2[\phi^{0'}(-\delta/2)^2 + \phi^{0''}(-\delta/2)] - \gamma_n + \delta\phi^{0'}(-\delta/2)\beta_n + \beta_n^2)\right]. \tag{A38}$$

2. *Maximum Small Signal Conductance for a One-Ion Channel Under Saturating Conditions*

In this appendix we find the ion–channel interaction potential that maximizes the small signal conductance of a one-ion channel under saturating conditions. The equation for the small signal conductance under saturating conditions (eqn 61) can be written:

$$G = \frac{4z^2e^2D}{k_bT\delta^2}\left[\int_{-1}^{1} e^{\phi(\delta v)}\, dv \int_{-1}^{1} e^{-\phi(\delta w)}\, dw\right]^{-1}. \tag{A39}$$

Maximizing G is equivalent to minimizing the double integral in the brackets. We rewrite this double integral as follows:

$$I(\phi) = \int_{-1}^{1}\int_{-1}^{1} e^{\phi(\delta v) - \phi(\delta w)}\, dv\, dw. \tag{A40}$$

$I(\phi)$ is composed of infinitesimal units of volume:

$$dV = e^{\phi(\delta v) - \phi(\delta w)}\, dv\, dw. \tag{A41}$$

We can construct $I(\phi)$ by combining pairs of elements dV. The pairs are chosen such that in one element $v = a$ and $w = b$, while in the other element $v = b$ and $w = a$. This pairing spans the entire region of integration by letting a and b vary from -1 to 1. Consider the elementary unit of volume composed of the sum of two such elements as follows:

$$dV_1 + dV_2 = [e^{\phi(\delta a) - \phi(\delta b)} + e^{\phi(\delta b) - \phi(\delta a)}]\, dv\, dw. \tag{A42}$$

This can be rearranged to yield:

$$dV_1 + dV_2 = 2\cosh[\phi(\delta a) - \phi(\delta b)]\, dv\, dw. \tag{A43}$$

Thus $I(\phi)$ is composed of elements of the form of eqn (A43). Clearly the entire volume is minimized if each element's volume is minimized. The minimum value of cosh is 1, thus the minimum volume of an element is $2dv\, dw$. This minimum occurs when the argument of cosh is 0. This can only occur if $\phi(\delta a) = \phi(\delta b)$ everywhere in the region of integration. Since a and b

are arbitrary, this requires that ϕ be a constant. This derivation does not determine the constant since G is independent of any offset in the potential. The value of this constant determines the concentration at which the channel is occupied half the time.

ACKNOWLEDGEMENTS

The authors gratefully acknowledge the many helpful suggestions made by Dr Eric Jakobsson and Dr Mitchell Watsky for his comments on the manuscript. Much of this work was done in partial fulfillment of the requirements for a Ph.D. in the Graduate Division of Physiology, Rush University. This work was supported by NIH grants EY03282, EY06005 and an unrestricted award from Research to Prevent Blindness to J. L. Rae and NIH grant GM 33816 and NSF grant DCB-8903795 to R. S. Eisenberg.

REFERENCES

ANDREOLI, T. E., HOFFMAN, J. F., FANESTIL, D. D. and SCHULTZ, S. G. (1986) *Physiology of Membrane Disorders*, 2nd edn, Plenum Medical Book Co., New York.

CHIU, S. W. and JAKOBSSON, E. (1989) Stochastic theory of singly occupied ion channels: II. Effects of access resistance and potential gradients extending into the bath. *Biophys. J.* **55**, 147–157.

CHIU, S. W., SUBRAMANIAM, S., JAKOBSSON, E. and MCCAMMON, J. A. (1989) Water and polypeptide conformations in the gramicidin channel. A molecular dynamics study. *Biophys. J.* **56**, 253–262.

COOPER, K. E., GATES, P. Y. and EISENBERG, R. S. (1988a) Surmounting barriers in ionic channels. *Q. Rev. Biophys.* **21**, 331–364.

COOPER, K. E., GATES, P. Y. and EISENBERG, R. S. (1988b) Diffusion theory and discrete rate constants in ion permeation. *J. membr. Biol.* **106**, 95–105.

DANI, J. A. (1989) Site-directed mutagenesis and single-channel currents define the ionic channel of the nicotinic acetylcholine receptor. *Trends Neurosci.* **12**, 125–128.

EDMONDS, D. T. (1989) A kinetic role for ionizable sites in membrane channel proteins. *Eur. Biophys. J.* **17**, 113–119.

EINSTEIN, A. (1926) *Investigations on the Theory of the Brownian Movement*, Dover Publications Inc., New York.

FRACE, A. M. and GARGUS, J. J. (1989) Activation of single-channel currents in mouse fibroblasts by platelet-derived growth factor. *Proc. natn. Acad. Sci. U.S.A.* **86**, 2511–2515.

FRIZZELL, R. A. (1987) Cystic fibrosis: a disease of ion channels? *Trends Neurosci.* **10**, 190–193.

FUROIS-CORBIN, S. and PULLMAN, A. (1989) Energy profiles in the acetylcholine receptor (AChR) channel: the MII–helix model and the role of the remaining helices. *FEBS Lett.* **252**, 63–68.

GARDINER, C. W. (1983) *Handbook of Stochastic Methods*, Springer-Verlag, New York.

GATES, P. Y., COOPER, K. E. and EISENBERG, R. S. (1990) Analytical diffusion models for membrane channels. In *Ion Channels*, Vol. II (ed. T. NARAHASHI), Plenum Press.

GOEL, N. S. and RICHTER-DYN, N. (1974) *Stochastic Models in Biology*, Academic Press, New York.

GOLDMAN, D. E. (1943) Potential, impedance, and rectification in membranes. *J. gen. Physiol.* **27**, 37–60.

HAINSWORTH, A. H. and HLADKY, S. B. (1987) Effects of double-layer polarization on ion transport. *Biophys. J.* **51**, 27–36.

HLADKY, S. B. (1984) Ion currents through pores: the roles of diffusion and external access steps in determining the currents through narrow pores. *Biophys. J.* **46**, 293–297.

HODGKIN, A. L. and KEYNES, R. D. (1955) The potasium permeability of a giant nerve fiber. *J. Physiol., Lond.* **128**, 61–88.

HOFFMAN, E. K. and SIMONSEN, L. O. (1989) Membrane mechanisms in volume and pH regulation in vertebrate cells. *Physiol. Rev.* **69**, 315–382.

JAKOBSSON, E. and CHIU, S. (1987) Stochastic theory of ion movement in channels with single-ion occupancy. *Biophys. J.* **52**, 33–45.

JORDAN, P. C. (1989) A molecular dynamics study of cesium ion motion in a gramicidin-like channel. Structural and energetic implications. In *Molecular Biology of Ion Channels* (eds. W. S. AGNEW, T. CLAUDIO and F. SIGWORTH), in press.

KRAMERS, H. A. (1940) Brownian motion in a field of force and the diffusion model of chemical reactions. *Physica* **7**, 284–304.

KREUGER, B. K. (1989) Toward an understanding of structure and function of ion channels. *FASEB J.* **3**, 1906–1914.

LAUGER, P. (1973) Ion transport through pores: A rate-theory analysis. *Biochim. biophys. Acta* **311**, 423–441.

LAUGER, P. (1976) Diffusion-limited ion flow through pores. *Biochim. biophys. Acta* **445**, 493–509.

LAUGER, P. (1985) Ionic channels with conformational substates. *Biophys. J.* **47**, 581–591.

LAUGER, P. (1988) Internal motions in proteins and gating kinetics of ionic channels. *Biophys. J.* **53**, 877–884.

LAVER, D. R., FAIRLEY, K. A. and WALKER, N. A. (1989) Ion permeation in a K^+ channel in *Chara australis*: direct evidence for diffusion limitation of ion flow in a maxi-K channel. *J. membr. Biol.* **108**, 153–164.

LEVITT, D. G. (1982) Comparison of Nernst-Planck and reaction-rate models for multiply occupied channels. *Biophys. J.* **37**, 575–587.

LEVITT, D. G. (1985) Strong electrolyte continuum theory solution for equilibrium profiles, diffusion limitation, and conductance in charged ion channels. *Biophys. J.* **52**, 575–587.

LEVITT, D. G. (1986) Interpretation of biological ion channel flux data. Reaction rate versus continuum theory. *A. Rev. Biophys. biophys. Chem.* **15**, 29–57.

LEVITT, D. G. (1987) Exact continuum solution for a channel that can be occupied by two ions. *Biophys. J.* **52**, 455–466.

LEVITT, D. G. (1989) Continuum model of voltage-dependent gating: macroscopic conductance, gating current, and single-channel behavior. *Biophys. J.* **55**, 489–498.

LEIBOVITCH, L. S., FISCHBARG, J. and KONIAREK, J. P. (1987) Ion channel kinetics: a model based on fractal scaling rather than multistate Markov processes. *Math. Biosci.* **84,** 37–68.

MILLER, C. (1989) Genetic manipulation of ion channels: a new approach to structure and mechanism. *Neuron* **2,** 1195–1205.

MILLHAUSER, G. L., SALPETER, E. E. and OSWALD, R. E. (1988) Diffusion models of ion–channel gating and the origin of power-law distributions from single-channel recording. *Proc. natn. Acad. Sci. U.S.A.* **85,** 1503–1507.

NUMA, S. (1989) A molecular view of neurotransmitter receptors and ionic channels. *The Harvey Lectures* **83,** 121–165.

PANDIELLA, A., MAGNI, M., LOVISOLO, D. and MELDOLESI, J. (1989) The effects of epidermal growth factor on membrane potential. *J. biol. Chem.* **264,** 12914–12921.

RIORDAN, J. R., ROMMENS, J. M., KEREM, B., ALON, N., ROZMAHEL, R., GRZELCZAK, Z., ZIELENSKI, J., LOK, S., PLAVSIC, N., CHOU, J. L., DRUMM, M. L., IANNUZZI, M. C., COLLINS, F. S. and TSUI, L. C. (1989) Identification of the cystic fibrosis gene: cloning and characterization of complementary DNA. *Science* **245,** 1066–1073.

SANDBLOM, J. (1985) Access permeability of ionic channels: dependence on aqueous jump distance. *Biophys. Chem.* **22,** 263–269.

WELSH, M. J. and FICK, R. B. (1987) Cystic fibrosis. *J. clin. Invest.* **80,** 1523–1526.

WOODBURY, J. W. (1971) Eyring rate theory model of the current–voltage relationships of ion channels in excitable membranes. In *Chemical Dynamics: Papers in Honor of Henry Eyring* (ed. J. O. HIRSCHFELDER), pp. 601–617, John Wiley, New York.